The Cryosphere Discuss., https://doi.org/10.5194/tc-2018-238
Manuscript under review for journal The Cryosphere
Discussion started: 12 November 2018

The Cryosphere Discussions
Open Access
EGU

High Mountain Asia glacier elevation trends 2003–2008, lake volume changes 1990–2015, and their relation to precipitation changes

Désirée Treichler[1], Andreas Kääb[1], Nadine Salzmann[2], and Chong-Yu Xu[1]

[1]Department of Geosciences, University of Oslo, Sem Sælands vei 1, 0371 Oslo, Norway
[2]Department of Geosciences, University of Fribourg, Chemin du Musée 4, 1700 Fribourg, Switzerland

Correspondence: Andreas Kääb (kaeaeb@geo.uio.no)

Abstract. We present an updated, spatially resolved estimate of 2003–2008 glacier volume changes for entire High Mountain Asia (HMA) from ICESat laser altimetry data. The results reveal a diverse pattern that is driven by spatially greatly varying glacier sensitivity, in particular to precipitation availability and changes. We introduce a spatially resolved zonation where ICESat samples are grouped into units of similar glacier behaviour, glacier type, and topographic settings. In several regions, our new zonation reveals local differences and anomalies that have not been described previously. A step-increase in precipitation around 1997–2000 on the Tibetan Plateau (TP) caused thickening of glaciers in the Eastern Pamirs, Kunlun Shan and central TP by 0.1–0.7 m a^{-1}. The thickening anomaly has a crisp boundary in the Eastern Pamir that continues just north of the central Karakoram. Glaciers in the south and east of the TP were thinning, with increasing rates towards southeast. The precipitation increase is reflected by growth of endorheic lakes in particular in the northern and eastern TP. We estimate lake volume changes through a combination of repeat lake extents from Landsat data and shoreline elevations from ICESat and the SRTM DEM for over 1300 lakes. The rise in water volume contained in the lakes corresponds to 4–25 mm a^{-1}, when distributed over entire catchments, for the areas where we see glacier thickening. The precipitation increase is also visible in sparse in-situ measurements and MERRA-2 climate reanalysis data, but less well in ERA Interim reanalysis data. Considering evaporation loss, the difference between average annual precipitation during the 1990s and 2000s suggested by these datasets is 34–100 mm a^{-1}, depending on region, which can fully explain both lake growth, and glacier thickening (Kunlun Shan) or glacier geometry changes (eastern TP). The precipitation increase reflected in these glacier changes possibly extended to the northern slopes of the Tarim Basin, where glaciers were nearly in balance in 2003–2008. Along the entire Himalaya, glaciers on the first orographic ridge, which are exposed to abundant precipitation, are thinning less than glaciers in the dryer climate of the inner ranges. Thinning rates in the Tien Shan vary spatially but are rather stronger than in other parts of HMA.

1 Introduction

High Mountain Asia (HMA) is a large and remote region hosting a range of topographic and meteoclimatic regimes (Palazzi et al., 2013). Some areas, like the Himalaya or Karakoram, are characterized by steep orographic gradients (Bolch et al., 2012). Glacier landscape and shapes, climate, elevation, and consequently glacier behaviour and response to climate change, vary strongly throughout the region (e.g. Scherler et al., 2011; Fujita and Nuimura, 2011; Bolch et al., 2012; Brun et al., 2017; Sakai

and Fujita, 2017). Throughout the recent decades, most glaciers in the region seem to have lost mass and retreated (e.g. Bolch et al., 2012; Kääb et al., 2012; Brun et al., 2017). But there are some exceptions, most prominent the so-called Karakoram anomaly (e.g. Hewitt, 2005; Quincey et al., 2011; Kääb et al., 2012; Gardelle et al., 2013; Kapnick et al., 2014), and positive mass balances are also reported for glaciers on the Tibetan Plateau (TP) and Kunlun Shan (Yao et al., 2012; Kääb et al., 2015; Brun et al., 2017).

At the same time, a number of studies report expansion of endorheic lakes on the TP from around the beginning of this century (e.g. Zhang et al., 2017). For these lake systems, additional lake water masses should either stem from increased lake inflow, i.e. mainly increased precipitation or enhanced glacier melt, or from reduced water loss, i.e. mainly changes in evaporation. However, in-situ meteorological data that could shed light on precipitation and evaporation changes and their spatial patterns is barely available for the HMA and lacking in particular for the remote areas on the TP and Kunlun Shan with suggested recent positive glacier mass balances. In addition, in-situ measurements at high altitude, in particular for precipitation, are in general subject to challenges (Salzmann et al., 2014). These scarceness and problems associated with in-situ measurements likely also affect the accuracy and reliability of reanalysis data over some zones of HMA, leaving thus an overall limited understanding of glacier changes and associated climate changes over significant areas of HMA.

HMA region-wide assessments of glacier changes have been derived either from (i) interpolating the sparse in-situ measurements (Cogley, 2011; Bolch et al., 2012; Yao et al., 2012), (ii) from digital elevation model (DEM) differencing (Gardelle et al., 2013; Brun et al., 2017), (iii) GRACE (Gravity Recovery and Climate Experiment) gravimetry data (Matsuo and Heki, 2010; Jacob et al., 2012; Gardner et al., 2013), or (iv) ICESat satellite laser altimetry (Kääb et al., 2012; Gardner et al., 2013; Neckel et al., 2014; Kääb et al., 2015; Phan et al., 2017). For some regions, the differences between the studies are considerable, even if they address the same time period (Cogley, 2012; Kääb et al., 2015). All four method principles listed above have their specific advantages and disadvantages. A challenge with GRACE data, for instance, is the separation of mass changes due to glacier mass loss and other influences, such as changes in lake and ground water storage (e.g. Baumann, 2012; Yi and Sun, 2014). For some DEM differencing studies in the region, a major source of uncertainties is the Shuttle Radar Topography Mission (SRTM) DEM. The SRTM DEM is based on C-band radar that can penetrate up to several metres into snow and ice, depending on the local snow and ice conditions during the SRTM data acquisition in February 2000 (Gardelle et al., 2012b; Kääb et al., 2015). The recent study of Brun et al. (2017) is not affected by radar penetration as it is exclusively based on time series from ASTER optical stereo DEMs. While their new data set of time-averaged geodetic glacier mass balances is spatially of unprecedented extent and detail, ASTER DEMs can suffer from limitations such as sensor shaking (jitter) (Girod et al., 2017), biased errors/voids in particular in featureless accumulation areas, and spatio-temporal variations in image acquisitions causing the studied time periods to vary throughout the area. With in-situ measurements and ICESat laser data, the uncertainty lies in the representativeness of the spatial sampling. Both are not spatially continuous but sample only some glaciers, although ICESat with higher density of footprints than in-situ measurements. Direct mass balance measurements are only available for few glaciers (WGMS, 2016, Fig. 1), and the overall mass balance signal they suggest is possibly biased towards glaciers at low elevations because these are easier to access (Wagnon et al., 2013).

The Cryosphere Discuss., https://doi.org/10.5194/tc-2018-238
Manuscript under review for journal The Cryosphere
Discussion started: 12 November 2018

From recent glacier studies involving ICESat data over HMA we conclude that results are sensitive to zone delineation, in particular in areas with strong spatial variability of glacier thickness changes (Kääb et al., 2015). Studies stress the importance of sampling the glacier hypsometry correctly. Kääb et al. (2012, 2015) and Treichler and Kääb (2016) found that hypsometries of individual years of ICESat samples may not fit the glacier hypsometry. This can alter the results in cases where there is a consistent elevation trend in 2003–2008 sampling elevations. Correct and up-to-date glacier outlines turn out to be very important for deriving ICESat elevation trends. Inclusion of non-glacier elevation measurements, where surface elevation is stable, reduces the glacier elevation change retrieved from ICESat. The effect of snow cover, and thus the choice of whether including ICESat winter campaigns or not, plays a role, not least for the autumn 2018 ICESat campaign (Kääb et al., 2012; Gardner et al., 2013; Treichler and Kääb, 2016). Spatially varying vertical biases from DEMs used as reference can considerably increase trend uncertainty (Treichler and Kääb, 2016). All ICESat studies in HMA so far rely on the SRTM DEM, where spatially varying penetration could be a source of such biases.

The present study has two objectives. First, we aim to extend the ICESat-based work of Kääb et al. (2012, 2015) to entire HMA, including the Tibetan Plateau, Qilian Shan and Tian Shan, and under special consideration of the issues addressed above and the recent method improvements by Treichler and Kääb (2016). In particular, we present a new elevation change zonation into spatial units that consider glacier topo-climatic setting, behaviour and type rather than relying on a regular grid or RGI regions. Second, we investigate the possible cause of the positive glacier volume changes in the TP and Kunlun Shan region, with the hypothesis of a precipitation increase in this area. For the latter purpose, we quantify the water volume changes in endorheic lakes on the TP, their timing and spatial pattern, and set them in relation to the independent ICESat-derived glacier volume changes as well as precipitation estimates from climate reanalyses and sparse in-situ measurements from meteorological stations. In order to avoid compiling spatially, temporally and methodologically inhomogeneous existing studies we prefer to derive integrated and consistent results, mainly based on ICESat data and satellite imagery.

2 Study region

HMA is covered by about 100'000 km^2 of glacier area (RGI, Arendt et al., 2015). Glaciers are found on all large mountain ranges around the TP at >4000 m a.s.l. but mostly to the south and west, where the steep elevation gradient from the Indian planes acts as a barrier for moisture that is advected by the Indian monsoon (Himalaya, Karakoram, Eastern Nyainqêntanglha Shan) and Westerlies (Hindu Kush, Karakoram, Pamir), respectively (Yao et al., 2012; Bolch et al., 2012; Mukhopadhyay and Khan, 2014). On the very dry TP, glaciers occur only on the sparsely spread small mountain ranges. In interplay with the Siberian High further north (Narama et al., 2010; Böhner, 2006), the Westerlies are the dominant source of moisture for the mountains surrounding the dry Tarim basin (at ca. 1000 m a.s.l.) — the Tian Shan to the north, and Kunlun Shan to the south (Ke et al., 2015a; Yao et al., 2012). The mountain ranges at the eastern margins of the TP (Qilian Shan, Hengduan Shan, Minya Gongga) are also influenced by the East Asian Monsoon (Yao et al., 2012; Li et al., 2015).

In both the monsoonal and westerly regimes, precipitation decreases northward (Bolch et al., 2012). Depending on the regionally dominant source of moisture, glacier accumulation happens at different times of the year (Bolch et al., 2012; Maussion

The Cryosphere Discuss., https://doi.org/10.5194/tc-2018-238
Manuscript under review for journal The Cryosphere
Discussion started: 12 November 2018

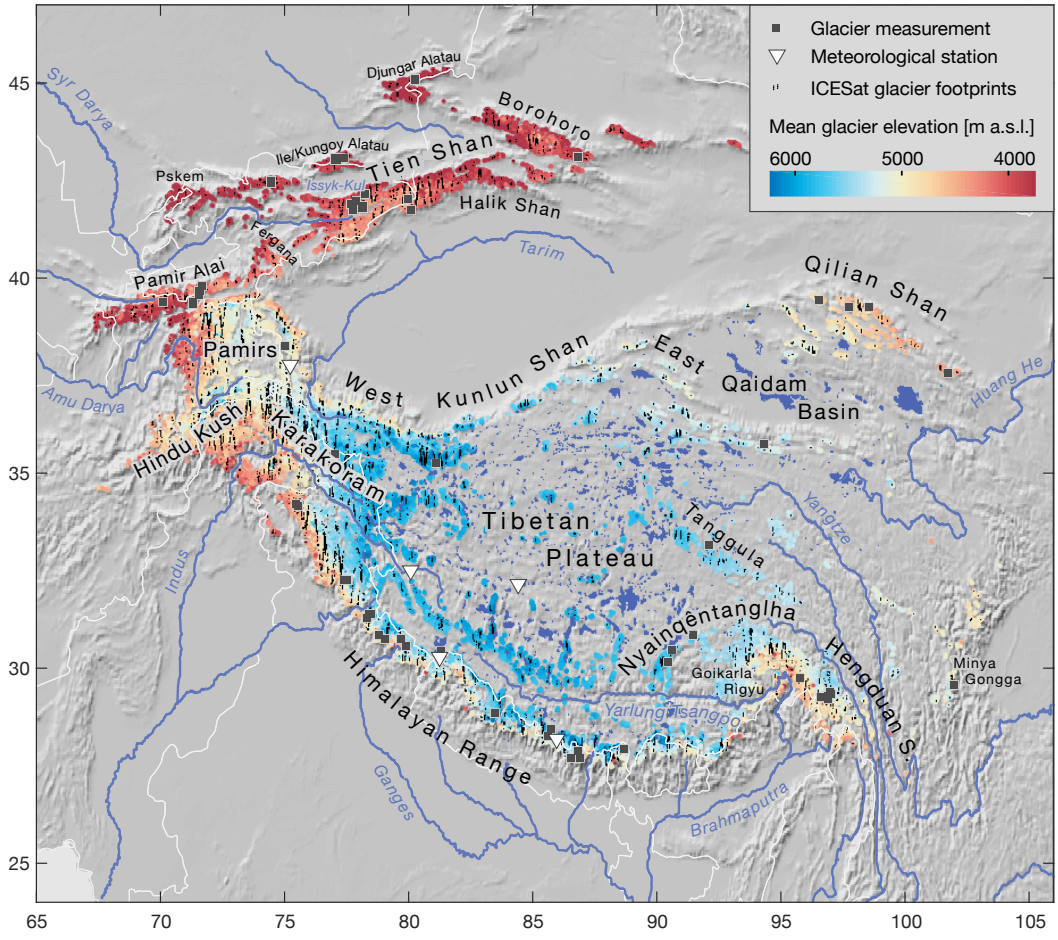

Figure 1. Mountain ranges and major rivers in High Mountain Asia, with meteorological stations used in this study (triangles) and in-situ glacier mass balance measurements done at some point during the last decades (black squares, WGMS, 2016). Lakes on the TP and in the Qaidam Basin are shown in dark blue, and glaciers are coloured according to their mean elevation. ICESat glacier samples are shown as small black dots. Glaciers taken from RGI.

et al., 2014; Yao et al., 2012; Sakai et al., 2015). From the eastern Himalaya and southern/eastern TP to the northwest of HMA, there is a transition from predominant spring/summer accumulation to winter accumulation in the Hindu Kush and the western parts of Tien Shan (Palazzi et al., 2013; Bookhagen and Burbank, 2010; Rasmussen, 2013). Mountains in between, such as the Karakoram and western Himalaya, receive moisture from both sources (Kuhle, 1990; Bolch et al., 2012). The Kunlun Mountains, on the other hand, receive most precipitation around May (Maussion et al., 2014). The seasonal timing of glacier accumulation likely plays an important role for glacier sensitivity to a warming climate (Fujita, 2008; Mölg et al., 2012; Sakai and Fujita, 2017). Another important factor is total precipitation availability, which depends on continentality (Shi and Liu, 2000; Kuhle, 1990) and, on smaller spatial scale, on glacier location on or behind a mountain range that acts as a primary

orographic barrier. Wagnon et al. (2013) and Sherpa et al. (2016) found indications of steep horizontal precipitation gradients within only a few kilometres on the outermost ridge of the Great Himalaya in the Khumbu region in Nepal. Vertical precipitation gradients at high altitude are still poorly understood. It is suggested that precipitation increases from dry mountain valley bottoms to an elevation of 4000–6000 m a.s.l. and subsequently decreases again at even higher elevations (e.g. Immerzeel et al., 2014, 2015).

Many glaciers in HMA are debris-covered in their ablation areas, and the percentage of debris-covered ice varies greatly between different regions (Scherler et al., 2011; Gardelle et al., 2013). Recent studies have found that although debris-covered glaciers in HMA have stable front positions (Scherler et al., 2011), they melt on average just as fast as clean ice glaciers (Kääb et al., 2012; Gardelle et al., 2012b; Pellicciotti et al., 2015). In this study, we distinguish thus not explicitly between debris-covered and debris-free glacier tongues.

3 Data and Methods

In this section we give a short overview of the data and methods used. Details can be found in the Appendix.

3.1 Data

For deriving repeat elevations on glaciers and lakes, we use data from the NASA Geoscience Laser Altimeter System (GLAS) aboard the Ice, Cloud and land Elevation Satellite (ICESat) that measured the Earth's surface elevations in two to three campaigns per year from 2003 to 2009. The campaigns were flown in northern autumn (∼ October–November), winter (∼ March), and early summer (∼ June). (Appendix A1).

As reference DEM for our ICESat processing and to derive lake shoreline elevations we use the DEM from the Shuttle Radar Topography Mission. We used the C-band, non-void-filled SRTM DEM version at 3 arc-seconds resolution (SRTM3). As an alternative elevation reference, we used also the SRTM DEM at 1-arc-second resolution (SRTM1). We did not explore or use the recently published TanDEM-X global DEM as it was not yet available during our processing. Due to temporal inconsistency and substantial voids, we did also not use the ALOS PRISM World DEM (AW3D) or the WorldView satellite optical stereo HMA DEM. (Appendix A2).

As an estimate for regional and temporal precipitation patterns for the years 1980–2015 we use data from the Modern-Era Retrospective analysis for Research and Applications, version 2 (MERRA-2), available from the NASA Goddard Earth Sciences Data and Information Services Center, and ERA Interim at T255 spectral resolution. We use monthly summarised values of the variables total precipitation (PRECTOT / tp), snowfall (PRECSNO / sf) and evaporation (EVAP / e) from MERRA-2's surface flux diagnostics dataset tavg1_2d_flx_Nx and ERA Interim's Monthly Means of Daily Forecast Accumulations, respectively. The High Asia Reanalysis (HAR), a product optimised for the TP region and with much finer spatial resolution, is unfortunately only available for the time period 2001–2011 which is too short for our study with respect to the lake volume changes investigated. Further, we use in-situ data from the five westernmost meteorological stations on the TP and Kunlun Shan

(Fig. 1), provided by the China Meteorological Science Data Sharing Service Network. The data includes daily measurements of precipitation, mean air temperature, and for the four stations on the southwestern TP also evaporation. (Appendix A3).

We extract repeat lake coverage from the Global Surface Water dataset that is a classification of the entire Landsat archive into monthly and annual maps of surface water. The data is available within Google Earth Engine. Coverage is nearly complete (>98%) starting from 2000 but considerably worse for some years of the 90s. (Appendix A4).

3.2 Methods for glacier volume change

We follow the double-differencing method explained in further detail in Kääb et al. (2012) and Treichler and Kääb (2016), with special consideration of issues mentioned in the above introduction. The difference between ICESat and SRTM elevations is further referred to as dh. Double differencing, i.e. fitting a linear trend through dh from several years, reveals how much the surface elevation has changed on average over the time period studied. We used only samples from ICESat's 2003–2008 autumn campaigns to avoid bias from temporal variations in snow depths (see introduction). After filtering, 74'938 ice samples and about ten times as many land samples remain. Per spatial unit, we estimate glacier surface elevation change by fitting a robust linear regression through individual dh and also compute a t-fit (Treichler and Kääb, 2016) and a non-parametric Theil-Sen linear regression (Theil, 1950; Sen, 1968). Our final estimate per spatial unit corresponds to the average of the three trend methods. (Appendix B)

ICESat data needs to be grouped into spatial units to fit surface elevation trends. We tested automated clustering methods from ICESat dh directly, but were not successful. We therefore preferred to delineate spatial units manually, considering topographic and climatic setting, elevation, visual glacier appearance, and input from literature and discussions with experts. In particular, we paid attention to orographic barriers. The zonation we present here is thus the result of an iterative manual process of re-defining spatial units until they yielded statistically stable and robust glacier surface change estimates. While the procedure is based on carefully applied expert knowledge, we are fully aware that our zonation is eventually a subjective one and certainly open to discussion. As a control approach, we applied the same gridding method as Kääb et al. (2012, 2015) to the entire HMA. (Appendix B1)

It is very important to ensure ICESat's elevation sampling is consistent through time and representative for glacier hypsometry (see introduction). We apply four different ways of correcting hypsometry mismatches of ICESat sampling. Our 'standard method' for the final glacier elevation change estimates corresponds to the average of all hypsometry-correcting methods and trend methods (robust, t- and Theil-Sen trends). Additionally, we also compute trends for only the upper/lower 50% glacier elevations as from RGI hypsometries (samples above/below the median RGI glacier elevation in each unit). The latter analysis violates mass conservation and should thus not be interpreted in terms of mass balance, but rather, for instance, for changes in glacier elevation gradients (e.g. Brun et al., 2017; Kääb et al., 2018). (Appendix B2)

Glacier elevation difference dh may be subject of vertical bias originating from local reference elevation bias or snow fall during the second part of the autumn 2008 campaign. Local vertical bias may result from inconsistent reference DEM age or production, tiling and tile/scene misregistration, or locally varying radar penetration (in case of the SRTM DEM). To remove this bias, we compute a per-glacier elevation correction cG corresponding to the median dh for each glacier, according to the

method described in Treichler and Kääb (2016). Treichler and Kääb (2016, 2017) found that ICESat clearly records the onset of winter snowfall in Norway during the split autumn 2008 campaign (stopped half way in mid-October and completed only in December). Analogue to Treichler and Kääb (2016), we estimate December 2008 snow bias from a linear regression of October/December 2008 land dh on elevation and time. (Appendix B3)

3.3 Methods for lake volume change

In order to relate glacier changes and precipitation changes on the Tibetan Plateau to each other, and in particular to investigate if precipitation increases could be a reason for the positive glacier mass balances found in parts of the region, we also derive the volume changes of endorheic lakes on the TP. On first order, and by neglecting changes in subsurface water transport, additional lake water masses should for endorheic lake systems either stem from increased lake inflow (mainly increased precipitation or enhanced glacier melt) or from reduced water loss (mainly changes in evaporation). Lake volume changes on the TP serve thus as potential proxies for precipitation changes, but help also to correct satellite gravimetric signals of glacier mass changes (see introduction; Appendix C).

We compute annual water volume change of the Tibetan lakes by multiplying annual lake areas with water level changes from repeat water surface elevations for each year over the period 1990–2015. Maximum annual lake extents are obtained directly from the Global Surface Water data set. We retrieve the corresponding lake surface elevations in two ways: a) from SRTM DEM elevations of the lake shore by computing the median of interpolated DEM elevations for lake shore cells for each areal extent, and b) directly from ICESat footprint elevations on the lake areas for those lakes where ICESat data is available. To extend the lake elevation time series from method b) beyond the ICESat period of 2003–2009, we compute the area–surface-elevation relationship for each lake by robust linear regression and apply this function to the areal extends of the years before and after the ICESat period. The so-extrapolated surface elevation values generate complete 1990–2015 time series for both areal extent and lake levels from SRTM and ICESat data, respectively. Our method is in parts similar to the methods used by previous studies but the inclusion of a DEM for deriving shoreline elevations, and thus lake water levels, in addition to altimetry data enabled us to produce volume change time series for one order of magnitude more lakes (>1300) than derived previously. (Appendix C).

To minimise the effect of uncertainties in or erroneous estimates for individual years, we analyse time series in a summarised way through regression over time and as decadal averages, and apply a range of filters. (Appendix C1).

To estimate the lake water volume change in a way that can be related to glacier mass balances and precipitation changes (i.e. mm w.e. per m^2), we summarise and spatially distribute the water volume changes of all lakes within spatially confined basins. These basins are based on endorheic catchments, but because many catchments only contain a single lake and exact catchment areas are not well defined on the TP (e.g., in very flat areas), we manually controlled, adjusted and aggregated the endorheic catchments of the USGS HydroSHEDS dataset at 15 arcsec spatial resolution to larger basins of comparable size and consisting of in average 5 catchments. (Appendix C2).

The Cryosphere Discuss., https://doi.org/10.5194/tc-2018-238
Manuscript under review for journal The Cryosphere
Discussion started: 12 November 2018

3.4 Methods for precipitation change

A change in precipitation, minus the part that is lost through evaporation and when neglecting changes in subsurface water transport, should yield numbers that are directly scalable in relation to endorheic catchment water volume change or glacier mass balance, especially where the latter is governed by precipitation rather than temperature/melt. However, reanalysis data may not be very accurate in HMA due to a lack of ground measurements, and the few meteorological stations are not necessarily representative for a larger area. We therefore use raw precipitation data mainly to detect/confirm temporal and large-scale spatial patterns, and in a summarised way through decadal averages, rather than relying on annual numbers.

4 Results

4.1 Glacier thinning and thickening

Figure 2a shows the 100 spatial units of glacier surface elevation change that result from the iterative manual zone delineation process. Spatial units needed to be large on the TP where glacier density is low, and could be rather small in the Karakoram which is intensely glacierised. Along major ridges such as the Himalaya, the units were designed narrow and along ridge orientation in order to group glaciers under similar temperature and precipitation regimes rather than across orographic barriers.

Surface elevation change for the new spatial units and the $2° \times 2°$ grid in Fig. 2b are derived using the 'standard method' (Appendix B) except for 34 units with hypsometry missampling or elevation bias. The error values given in Fig. 2c and in the text conservatively include, where applicable, uncertainties from off-glacier elevation trends, the deviation from the standard method (greatly increased errors, units showing up in yellow in Fig. 2c), and the difference to the surface elevation change rate corrected for the effect of December 2008 snow fall. In areas with snow-rich winters, the latter may contribute up to 40% of the error budget. In Fig. 2b, the size of the circles corresponds to the number of samples (minimum 200) while the overlaid, grey circles show the trend error (at 1σ) in relation to the trend slope; i.e. trends are not statistically significant different from zero where the grey circles fully cover the underlying coloured circle. Errors for 2a are given in Fig. 2c.

The overall pattern of elevation change is the same for both spatial zonation approaches; positive glacier elevation change in the Kunlun Shan an the inner TP, and spatially varying but modest glacier surface lowering in most areas except for very negative values in Nyainqêntanglha Shan/Hengduan Shan and parts of the Tien Shan. While the grid zonation shows smooth transitions between areas of positive or negative glacier evolution, our zoned map suggests rather greater spatial variability and sharper boundaries of clusters of similar elevation change. The regular grid size is too small to reach minimum sample numbers in areas with sparse glacier coverage (TP, outer Hengduan Shan, parts of Tien Shan), and the signal from grid cells with few samples is spatially less consistent than what the manually delinated, larger units suggest. The small units in the Karakoram and Kunlun Shan, on the other hand, reveal locally varying signals that are averaged out or not significant in the coarser grid zonation (e.g. units K1–K3 and KS1 in Fig. 2a).

In the Himalaya, the manual zone delineation shows a clear transition from moderately negative elevation change on the first, southern orographic ridge (-0.15 to $-0.34\,\mathrm{m\,a^{-1}}$, maximum trend error: $0.31\,\mathrm{m\,a^{-1}}$) compared to glaciers located further back

The Cryosphere Discuss., https://doi.org/10.5194/tc-2018-238
Manuscript under review for journal The Cryosphere
Discussion started: 12 November 2018

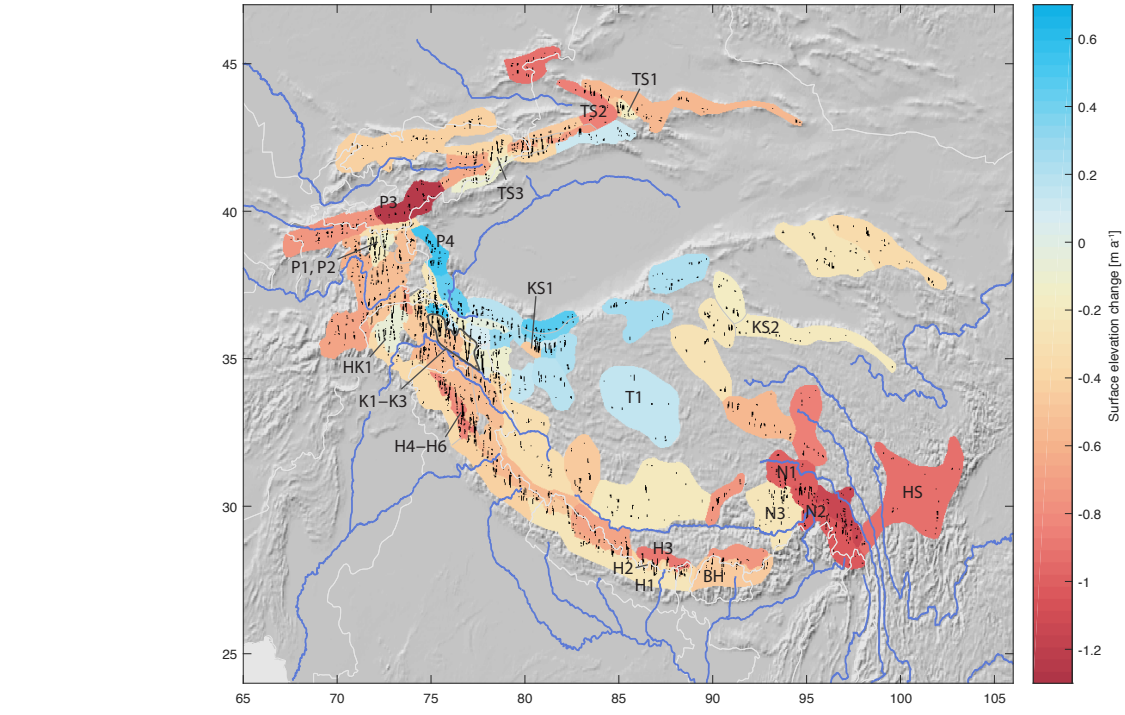

(a) Zonal glacier elevation change

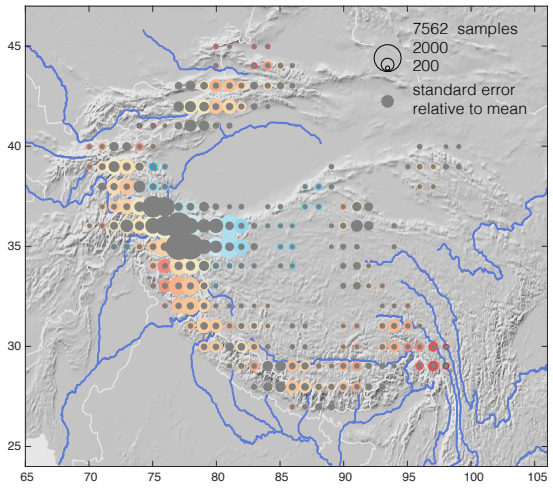

(b) Gridded glacier elevation change

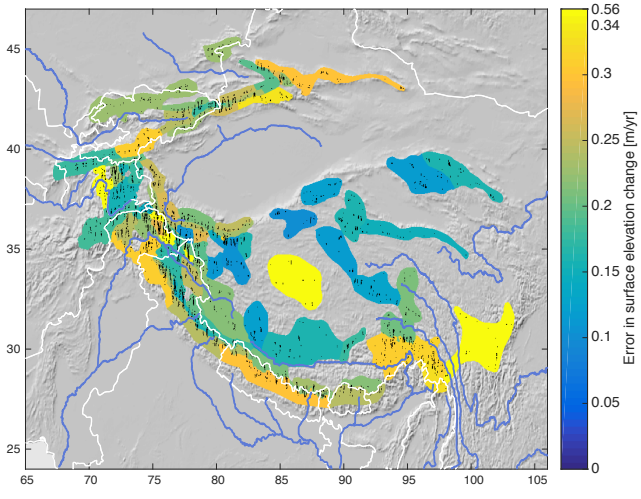

(c) Errors for zonal elevation change

Figure 2. 2003–2008 glacier elevation change rates for (a) manually delineated zones and (b) overlapping 2° × 2° degree grid cells with 1° spacing. Colour bar (b) as in (a). Circles in (b) are scaled according to sample numbers. The overlaid grey circles show the standard error in relation to the slope of the linear fit, i.e. elevation change is not significantly different from zero (at 1σ) where the coloured circles are fully covered. (c), Error for (a) at 1σ, including uncertainties from deviations from the standard method, December 2008 snow fall correction, and trends in off-glacier samples. The four bright yellow units have uncertainties between 0.42–0.56 m a^{-1}.

The Cryosphere Discuss., https://doi.org/10.5194/tc-2018-238
Manuscript under review for journal The Cryosphere
Discussion started: 12 November 2018

to the north and on the edge of the TP ($-0.33 \pm 0.22\,\mathrm{m\,a^{-1}}$ to $-0.85 \pm 0.14\,\mathrm{m\,a^{-1}}$). This pattern (e.g. units H1, H2, H3) is consistent along the entire range except for the Bhutanese Himalaya, where ICESat's sampling pattern required grouping of several orographic ridges which together show stronger surface lowering (unit BH, $-0.40 \pm 0.25\,\mathrm{m\,a^{-1}}$). This pattern becomes smoothed out and is thus not visible in the gridded zonation.

Glaciers in the inner Hindu Kush (HK1, $0.03 \pm 0.24\,\mathrm{m\,a^{-1}}$) and the highest regions of the Pamir (P1 -0.07 ± 0.23, P2 $-0.03 \pm 0.16\,\mathrm{m\,a^{-1}}$) were close to balance over 2003–2008 while all surrounding units in the area show stronger glacier surface lowering. Similarly, the glaciers around Lhasa (Goikarla Rigyu, unit N3) lowered their surface by only $-0.18 \pm 0.31\,\mathrm{m\,a^{-1}}$ which is considerably less than the surrounding units and in particular the very negative values in East Nyainqêntanglha Shan/Hengduan Shan (-0.96 to $-1.14 \pm 0.33\,\mathrm{m\,a^{-1}}$).

Further towards the inner TP and in the Qilian Shan, surface lowering decreases to -0.1 to $-0.3 \pm 0.16\,\mathrm{m\,a^{-1}}$. In the central and northern parts of the TP and the Kunlun Shan it turns positive — for nearly all units $> 0.25\,\mathrm{m\,a^{-1}}$, to as much as $0.79 \pm 0.26\,\mathrm{m\,a^{-1}}$ in the Eastern Pamirs/Kongur Shan (P4). The boundary between positive and negative surface elevation change seems to be formed by the Muji Basin, upper Gez river and Tashkurgan Valley. All units to the north of the central Karakoram range were in balance or thickening. The glaciers of the central Karakoram range and southwest of it showed moderate thinning (-0.22 to $-0.51 \pm 0.43\,\mathrm{m\,a^{-1}}$). In the Western Kunlun Shan region, surface elevation trends of the lower 50% elevations are more positive than those of the upper 50% elevations (not shown). This behaviour is visible for 13 units centred around KS1.

Interestingly, also glaciers on the northern edge of the Tarim basin seem to be closer to balance (-0.3 ± 0.26 to $+0.21 \pm 0.33\,\mathrm{m\,a^{-1}}$) than those in more central or northern ridges of the Tien Shan. In the Tien Shan, most spatial units indicate glacier surface lowering between -0.35 and $-0.8 \pm 0.25\,\mathrm{m\,a^{-1}}$, but two units stick out due to their more moderate surface lowering; TS1: $-0.1 \pm 0.21\,\mathrm{m\,a^{-1}}$, and TS3: $-0.18 \pm 0.18\,\mathrm{m\,a^{-1}}$. Several other units right next to these have considerably more negative values. At the transition between Pamir and Tien Shan (P3), glacier surface elevation decreased by as much as $-1.23 \pm 0.31\,\mathrm{m\,a^{-1}}$ — despite the thickening signal just south and east of this unit.

4.2 Influence of dh–elevation gradient and December 2008 snow fall

The dh–elevation gradients between ICESat and the SRTM DEM are in some units very steep (Fig. 3d). Steep dh–elevation gradients can result from altitudinal trends in radar penetration or glacier geometry changes between SRTM and ICESat surface elevation acquisitions. The steeper dh–elevation gradients are, the stronger is the biasing influence from glacier hypsometry missampling. On the TP and in the northern and eastern ranges of the Tien Shan, the gradients range between 1.5–2.5 m per 100 m elevation. Glaciers in these areas typically occur within an elevation range of ca. 1000 m. In the Nyainqêntanglha Shan/Hengduan Shan, West Kunlun Shan, Karakoram, southwestern Tien Shan and the highest Pamir mountains, dh–elevation gradient values are 1–1.5 m per 100 m elevation. The gradients are moderate (< 1 m per 100 m elevation) in the Himalaya, East Kunlun Shan, lower in Pamir, and lowest in the Hindu Kush (0.14 m per 100 m). Our method ensures that any bias from inconsistent sampling of glacier elevations for individual ICESat campaigns is corrected. Neglecting the effect of glacier

The Cryosphere Discuss., https://doi.org/10.5194/tc-2018-238
Manuscript under review for journal The Cryosphere
Discussion started: 12 November 2018

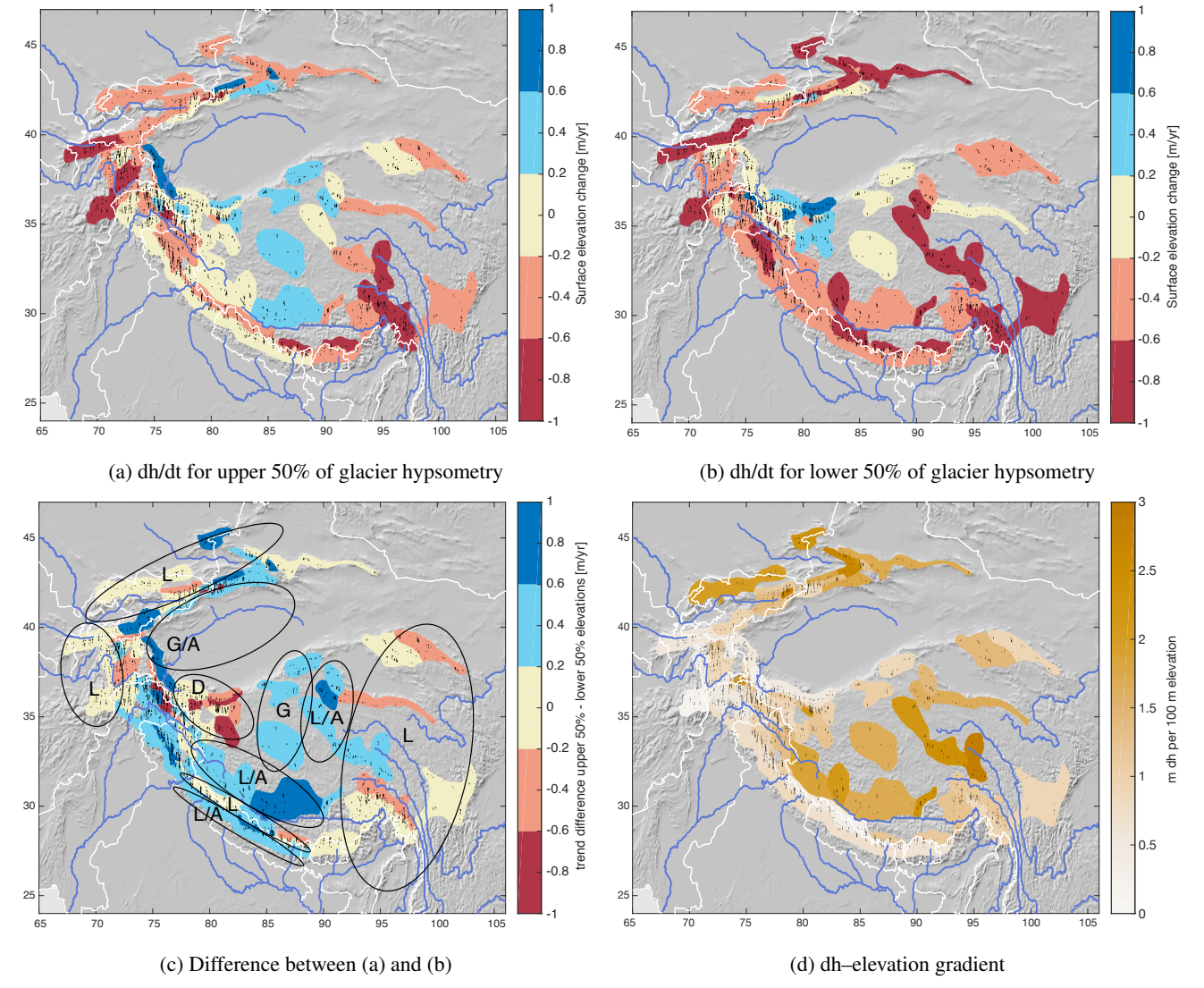

(a) dh/dt for upper 50% of glacier hypsometry

(b) dh/dt for lower 50% of glacier hypsometry

(c) Difference between (a) and (b)

(d) dh–elevation gradient

Figure 3. Glacier accumulation and ablation areas indicate regionally different, distinct glacier evolution: glacier surface elevation change for (a) upper 50% and (b) lower 50% of glacier hypsometry, and (c) the difference of the two (upper minus lower). The letters indicate: L – thickness loss on entire glacier, G – thickness gain, A – adjusting glacier geometry with thinning ablation areas, D – dynamic adjusting of glacier geometry with thickening ablation areas. (d) Gradients of dh (ICESat–SRTM surface elevation) with elevation. Steep dh–elevation gradients may be caused by high SRTM penetration depths in dry, cold accumulation areas and/or from glaciers adjusting their geometry.

hypsometry missampling or a trend in sampled glacier elevations would result in considerable bias: on average $\pm 0.13\,\mathrm{m\,a^{-1}}$, but exceeding $0.1\,\mathrm{m\,a^{-1}}$ in 51 of 100 units. The most extreme cases ($> \pm 0.3\,\mathrm{m\,a^{-1}}$) are three units each in Tien Shan and Karakoram.

The Cryosphere Discuss., https://doi.org/10.5194/tc-2018-238
Manuscript under review for journal The Cryosphere
Discussion started: 12 November 2018

Correcting dh retrieved from the December 2008 campaign for the effect of increasing snow cover has an unexpectedly large influence on glacier surface elevation change rates. Elevation trends from corrected dh are on average 0.088 m a^{-1} more negative/less positive. The maximum effect of the December 2008 correction is as much as -0.25 m a^{-1} (in unit N2; for off-glacier samples: -0.11 m a^{-1} in unit H2), which is of considerable size given that it is caused by only ca. 10% of all samples (half of one of five campaigns). The potential biasing effect is in fact greatest in areas where MERRA-2 data suggests snow fall during October/November/December 2008 and where off-glacier samples suggest a positive surface change trend. However, in 20 out of 100 units we were not able to compute the potential biasing effect of December 2008 snow cover (e.g., due to lack of off-glacier samples). To ensure a consistent approach, we did therefore not apply this correction to the results presented above but instead added the difference due to bias correction to the error budget.

4.3 Lake changes on the TP

We receive valid (according to our filter procedures) water volume change time series for 89% of the median lake area (74% of all endorheic lakes) on the TP: 1009 lakes with SRTM-based lake surface elevations, thereof 103 also having ICESat-based lake surface elevations (59% of the lake area). Extrapolated lake levels based on annual or campaign ICESat data yield the same results, but ICESat-based lake level change is on average 1.55 times larger than SRTM-based values. Multiplied with areal changes to receive volume changes, the relative difference is reduced to 1.09 times. Average 1990–2015 lake growth corresponds to 0.14 m a^{-1} (SRTM) and 0.18 m a^{-1} (ICESat) in lake-level change per year (Fig. 4a, robust linear regression of dV scaled with median lake area for easier comparison of values between lakes of very different size). All, except a handful of lakes predominantly in the very south of the TP, grew during the studied time period, and growth of individual lakes is largest in the northern and eastern part of the TP. Figure 5 shows relative lake volume growth (based on SRTM lake levels) for individual lakes and regional medians over time for six regions: southwestern, eastern, central, northeastern, northwestern TP and Qilian Shan, indicated in Fig. 4a. (Note that the y-axis in Fig. 4a is relative to the total volume change dV over the time period observed and does not show absolute lake volumes; these are unknown as our method only detects lake level changes and not lake depths). Rather than growing steadily, most lakes seem to have undergone a phase of sudden and rapid growth starting in ∼1997 and gradually slowing down until ∼2009, with rather stable conditions before and after this period. Relative lake volume change was most sudden and rapid for the northeastern, northwestern, central and eastern TP (the former three corresponding to areas with 2003–2008 glacier thickening). Lakes in the southern and southwestern part of the TP showed more varying and overall less growth, with a tendency to decrease after 2010. Endorheic lakes in the Qaidam basin/Qilian Shan region further northeast also show a different and more varying evolution with slower growth that started only around 2004, but continued until ∼2012. The latter effect is also visible for the adjacent lakes on the northeastern TP (east Kunlun Shan).

Figure 4b shows the corresponding specific annual water volume change per endorheic catchment as the decadal difference between 1990–1999 and 2000–2009 average lake volumes (based on SRTM lake levels). The pattern of predominant water volume increase especially in the northern and eastern TP compares well to the results in Fig. 4a but with a stronger accentuation of the lake volume growth on the eastern TP due to considerably larger lake areas and lake density compared to the mostly small lakes further north/west. Table 1 shows additional water volumes accumulated between the two decades for the same

The Cryosphere Discuss., https://doi.org/10.5194/tc-2018-238
Manuscript under review for journal The Cryosphere
Discussion started: 12 November 2018

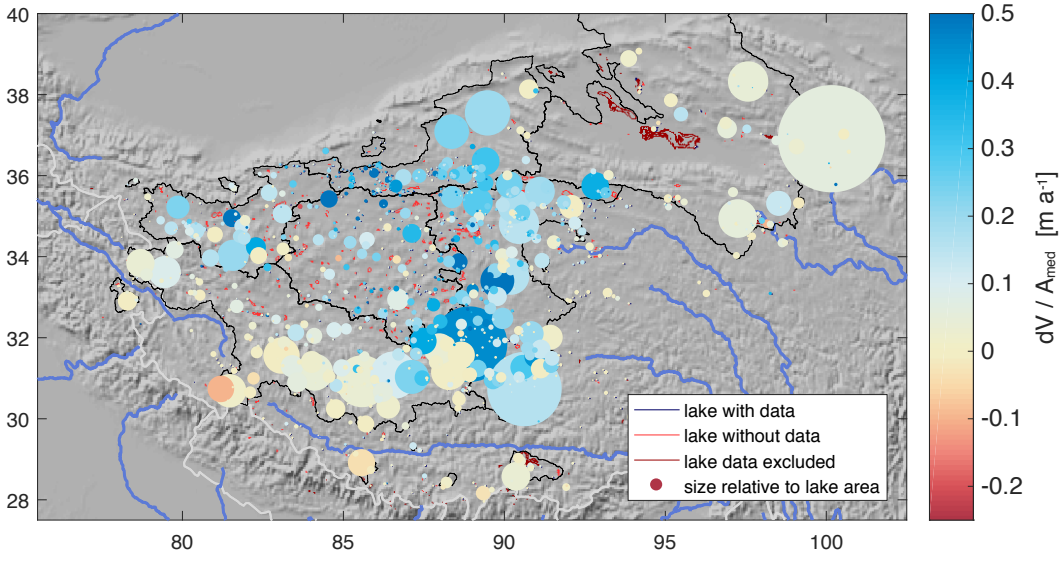

(a) Normalised 1990–2015 lake volume change for individual lakes

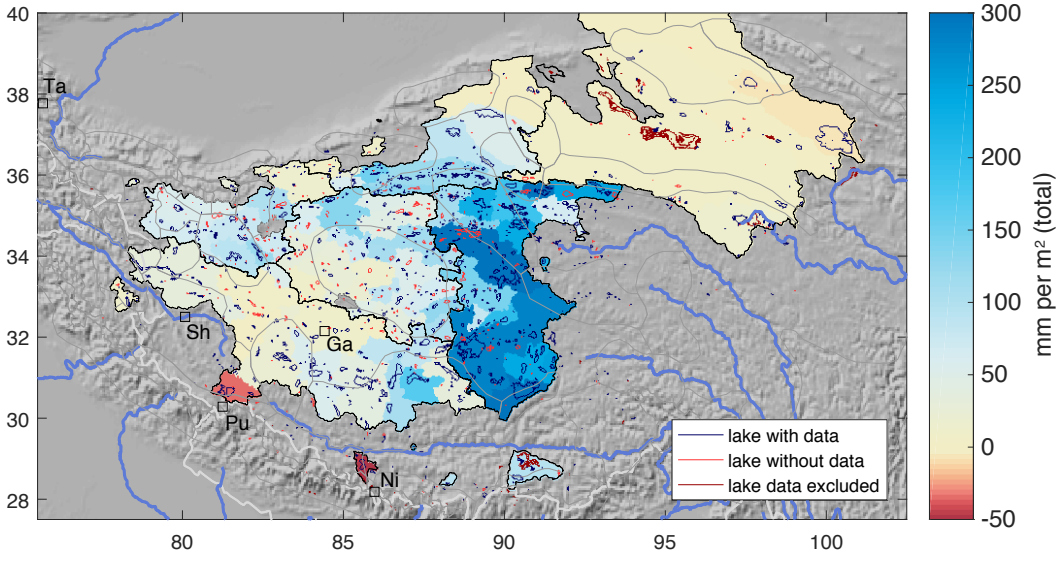

(b) Annual specific water change per endorheic catchment between 1990–1999 and 2000–2009

Figure 4. Lake volume changes on the Tibetan Plateau. (a) Normalised lake volume change for individual lakes. Colours show the average annual 1990–2015 lake level change in metres (volume change dV divided by median lake area to receive comparable values). Circles are scaled relative to lake area. (b) Annual specific water change per endorheic catchment for the decadal difference between 1990–1999 and 2000–2009 lake volumes. Values correspond to the sum of individual lake water volume changes (average changes assumed for lakes with missing data) divided by catchment area to make their units comparable to precipitation sums. Red lake outlines: lacking plausible data; purple lake outlines: lakes excluded due to human influence on lake levels/extent. Squares: meteorological stations. Regions with black outlines referred to in the text.

The Cryosphere Discuss., https://doi.org/10.5194/tc-2018-238
Manuscript under review for journal The Cryosphere
Discussion started: 12 November 2018

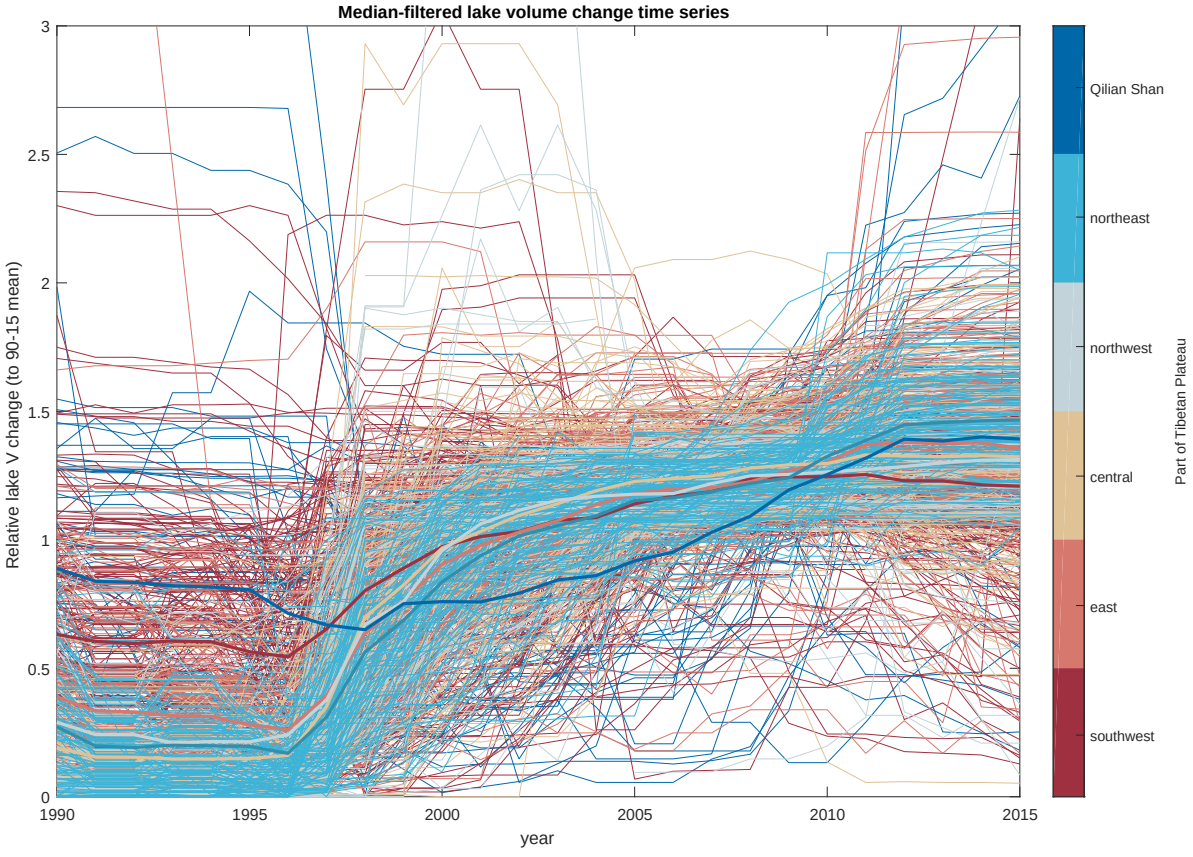

Figure 5. Relative lake volume change for individual lakes on the Tibetan Plateau, coloured by region. Volume changes dV are normalised by the 1990–2015 mean dV for comparability, annual values are median-filtered (7 years window size). Thick lines indicate the median for each region. The regions northeast, northwest and central correspond to areas with observed 2003–2008 glacier thickening.

regions as above. To yield values comparable to precipitation changes, the reader has to divide the total decadal differences dV given in the table by the number of years during which the additional water was accumulated. Assuming the change happened rather gradual during the entire decade, the specific annual water change would correspond to $1/10$ of the values in Table 1. For instance, for water volumes using SRTM-based lake levels: 25 ± 3 mm a^{-1} for the eastern TP, 4 ± 1 mm a^{-1} for the southwestern TP, 6–7 ± 1 mm a^{-1} for the central and northern TP, and 0.1 ± 0.5 mm a^{-1} for the Qaidam basin/Qilian Shan region. Notably, there are considerable differences between catchments within each region (range for SRTM-based estimates: –5 ± 1 to +35 ± 6 mm a^{-1}, excluding one outlier of 163 ± 7 mm a^{-1} for the catchment centred at 34.3° N / 88.8° E). The estimates based on SRTM- and ICESat lake levels aggregated for the six regions nevertheless agree very closely. The above annual values have to be doubled, or the dV values given in the table multiplied by $1/5$, for instance, if one prefers to assume that the water

The Cryosphere Discuss., https://doi.org/10.5194/tc-2018-238
Manuscript under review for journal The Cryosphere
Discussion started: 12 November 2018

Table 1. Water volume changes between decadal averages of the 1990s and the 2000s, and 2003–2008 annual glacier mass balance of adjacent glacierised areas. dV: total decadal lake water volume difference in mm, dP: annual precipitation difference in mm a^{-1}, station order in southwest TP: Shiquanhe, Gaize, Pulan, Nielaer. Glacier surface elevation changes are converted to mm w.eq. a^{-1} assuming a density of 850 kg m^{-3}.

Region	dV SRTM	dV ICESat	dP MERRA-2	dP ERA Interim	dP stations	Glacier mass balance
Southwest TP	39±11	59±16	81±33	15 ± 31	−1 ± 14, 42±17, 19 ± 16, 60±50	−33 ± 11 to −10 ± 14
East TP	252±33	275±37	100±18	30 ± 14		−17 ± 10 to −8 ± 14
Central TP	69±10	71±11	56±5	25 ± 8		21 ± 38
Northwest TP	62±14	70±15	34±11	−33 ± 11	16 ± 72	29 ± 10 to 31 ± 9
Northeast TP	60±12	54±9	85±13	−2 ± 22		13 ± 11 to 50 ± 21
Qaidam / Qilian	1±5	1±4	87±14	24 ± 17		−25 ± 14 to −13 ± 10

volume increase happened during 5 years only, with stable conditions before and after — an assumption which seems also well plausible from Fig. 5.

4.4 Precipitation increase on the TP

Annual precipitation sums on the TP from meteorological stations range from as little as 50–100 mm a^{-1} (Shiqanhe and Thashkurgan stations, southwest TP and West Kunlun Shan) to 500–900 mm a^{-1} (Nielaer station, southern TP). Reanalysis values of both products used, MERRA-2 and ERA Interim, lie in between. All datasets record the majority of precipitation (>70%) during the monsoon-influenced summer months (May–September), except for Pulan and Nielaer, the two southernmost stations close to the Himalaya (only ca. 50% precipitation in summer).

Of the five meteorological stations available, especially Shiquanhe and Pulan show little change in precipitation and pan evaporation (Fig. 6). The Gaize station, located most central on the TP but still more south than our corresponding glacier unit, indicates a step-like precipitation increase around the year 2000, but data from only one station need of course to be interpreted with care due to potential local effects and changes to the station. A more gradual increase is visible in the Tashkurgan data. Differences in decadal average precipitation range from −1 (Shiqanhe) to 60 mm (Nielaer) within 10 years, notably with greatest relative change for the Gaize station (+42 mm per decade, a 25% increase) and Tashkurgan station (+16 mm or +22% per decade). Decadal differences are mostly (Nielaer, Tashkurgan) or exclusively (other stations) caused by an increase of precipitation during summer months. Pan evaporation reaches twice to tenfold of precipitation sums.

The two reanalyses used here differ considerably both in precipitation evolution and in estimated evaporation. Figures 8a (ERA Interim) and 8b (MERRA-2) show regional averaged annual sums for total precipitation, evaporation, and the difference of the two, for grid points within the TP lake catchment regions defined above. Notably, ERA Interim suggests considerably

The Cryosphere Discuss., https://doi.org/10.5194/tc-2018-238
Manuscript under review for journal The Cryosphere
Discussion started: 12 November 2018

higher evaporation values than MERRA-2, in particular for the southwestern TP and the three northern regions, resulting in much lower suggested net water availability in the areas where we see glacier thickening than it is the case for MERRA-2. Both reanalyses show an increase in precipitation starting from ca. 1995, but for ERA Interim, the evolution only lasts until ca. 2000 after which precipitation sums decrease. Also, the short-term precipitation increase is not visible for the northern parts of the TP, and it does not result in a noticeable decadal difference between average annual precipitation in 1990–1999 vs. 2000–2009.

MERRA-2, on the other hand, rather suggests a step-wise increase with continuously higher precipitation sums until ca. 2010 for the entire TP, and even a continuous increase through 2015 for the northern part of the TP. For all six regions, this results in a total increase in precipitation of 34 mm (northwestern TP) to 100 mm (eastern TP) mm within 10 years. Except for the Qilian Shan region, the change is exclusively driven by increasing summer precipitation (Fig. 7b). Winter precipitaion did not change noticeably (-9 to -2 mm decadal change for the five TP regions, $+8$ mm for Qilian Shan).

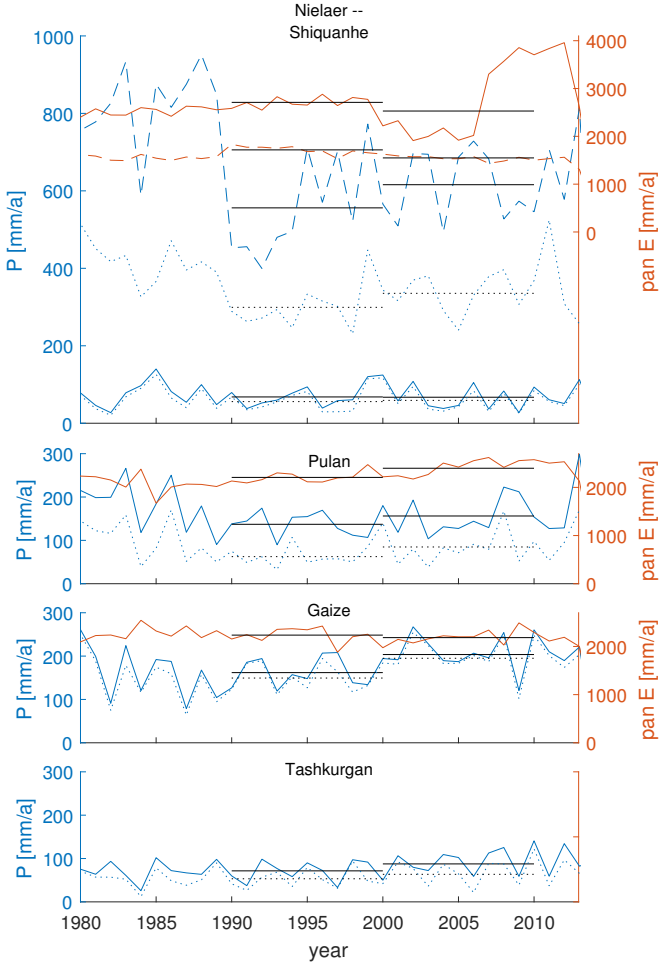

Figure 6. Annual precipitation (P, blue line), pan evaporation (pan E, red line), and summer precipitation (dotted lines) for five stations on the southern and western TP (Fig. 4b). The uppermost panel combines two stations (Nielaer: dashed lines; Shiquanhe: solid lines).

The Cryosphere Discuss., https://doi.org/10.5194/tc-2018-238
Manuscript under review for journal The Cryosphere
Discussion started: 12 November 2018

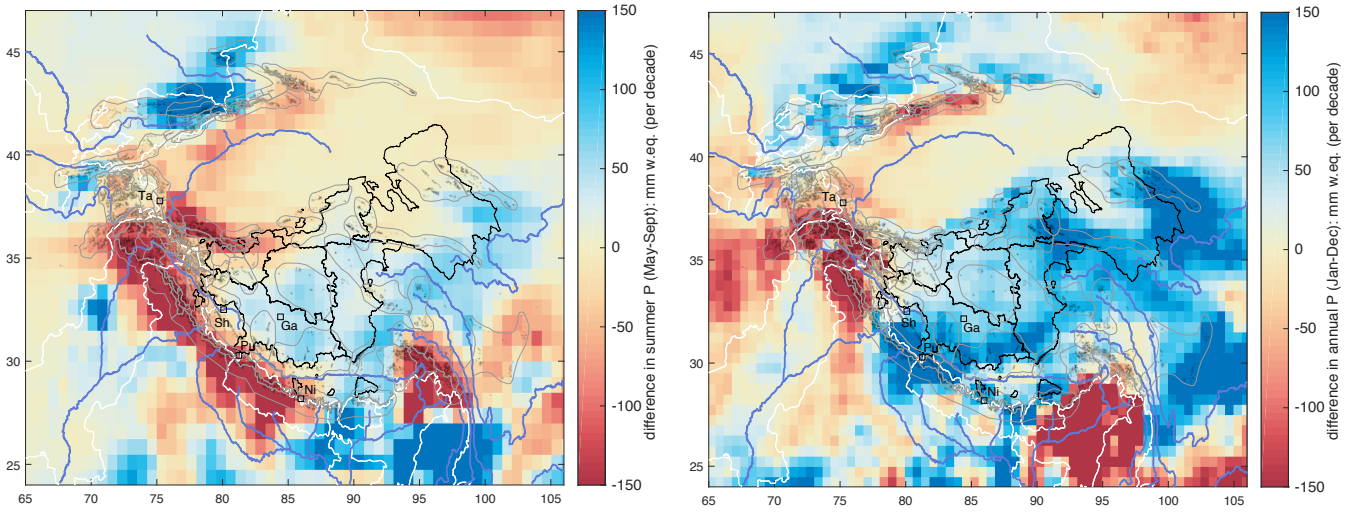

(a) ERA Interim (b) MERRA-2

Figure 7. Difference between decadal averages of summer precipitation (May–September) in 2000–2009 and 1990–1999. MERRA-2 suggests an increase of up to 100 mm within 10 years on the TP and in the Kunlun Shan, compared to only a slight increase on the TP and decreasing precipitation in the Kunlun Shan for ERA Interim.

The Cryosphere Discuss., https://doi.org/10.5194/tc-2018-238
Manuscript under review for journal The Cryosphere
Discussion started: 12 November 2018

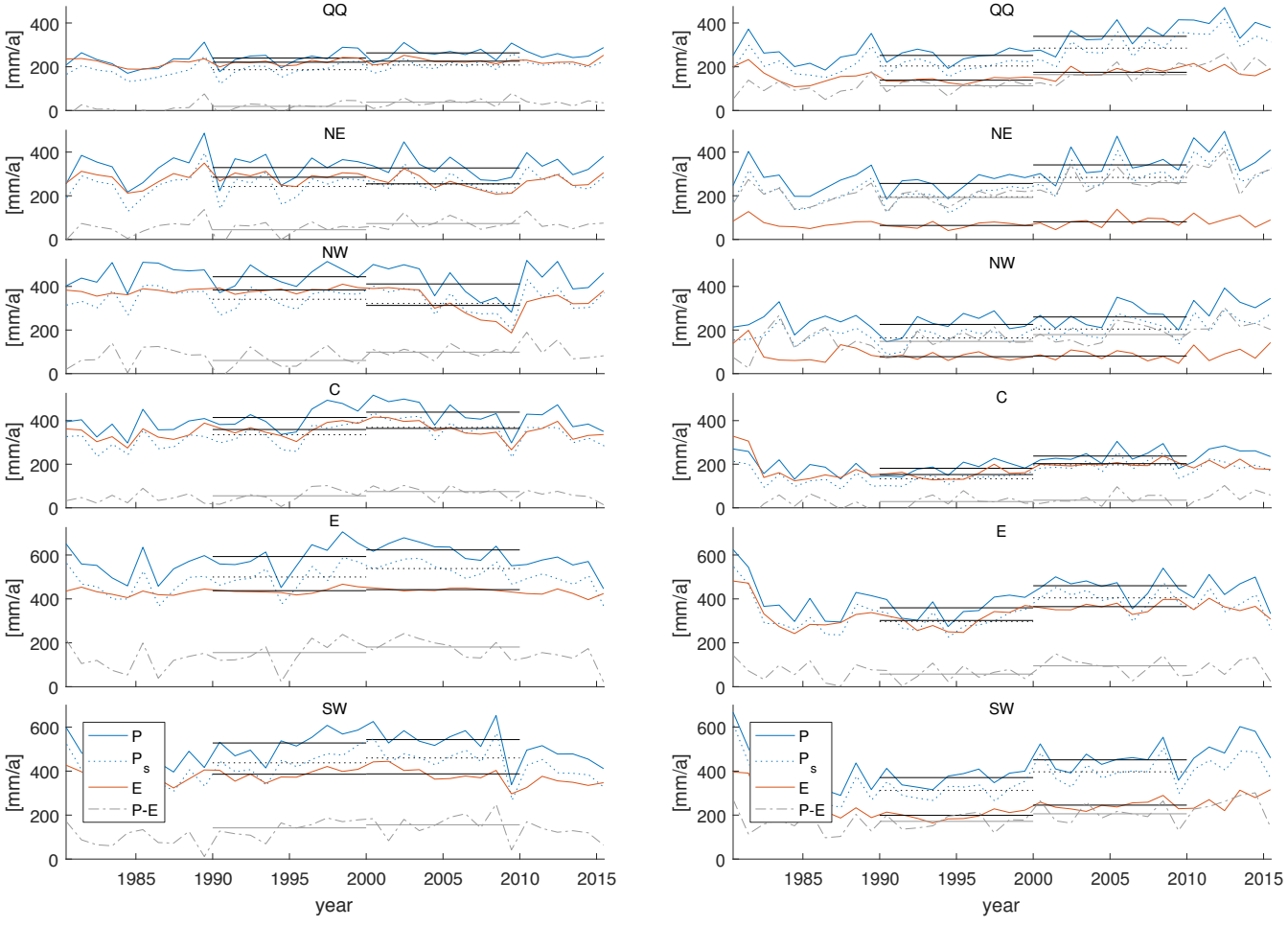

(a) ERA Interim

(b) MERRA-2

Figure 8. Timeseries of annual total precipitation (P), evaporation (E), the difference of the two (P-E), summer precipitation (Ps, May–Sept), and their respective decadal averages, for reanalysis grid points within the six lake change regions on the TP: southwestern (SW), eastern (E), central (C), northwestern (NW), northeastern (NE) TP and Qaidam Basin / Qilian Shan (QQ).

When correcting these values with MERRA-2 estimates of actual evaporation, the total decadal increase in water availability ranges from 6 mm (central TP) to 68 mm (northeastern TP). The evaporation-corrected increase is even greater when looking at summer months only (31–77 mm per decade, compared to a decrease in water availability during winter months of −27 to −6 mm, not shown). MERRA-2 suggests that 30–60% of precipitation on the TP falls as snow during the summer months and that the proportion of snow fall did not change noticeably between the decades (not shown).

The regions where MERRA-2 indicates increased summer precipitation correspond well with those areas on the TP and in Eastern Kunlun Shan with moderately negative to positive surface elevation change and/or endorheic lake growth. ERA Interim

data indicates a similar pattern but with much lower (TP) precipitation increase, or even decrease in case of the Kunlun Shan region (Fig. 7a)

Our above results on precipitation changes relate to decadal means in order to enable systematic comparison to other data. It is however important to note that these results vary if other time periods are chosen for aggregation. Kääb et al. (2018), for instance, summarize total annual precipitation amounts estimated from ERA-interim reanalysis over the Aru region, nortwestern TP, over 1979–1995 and 1995–2008 to suggest a 33% increase between the latter both periods.

5 Discussion

The 2003–2008 ICESat surface elevation changes paint a spatially diverse picture of glacier changes in HMA. The general pattern — glacier volume gain in the Kunlun Shan and the inner TP and glacier volume loss elsewhere — appears robust, no matter whether we aggregate the samples in a regular grid or manually delineated units. The more distinct spatial pattern agrees with the ICESat studies of Kääb et al. (2015, 2012), the ASTER-based geodetic mass balances of Brun et al. (2017) and with the overall picture drawn by the previous regional studies of Neckel et al. (2014), Gardner et al. (2013) and Farinotti et al. (2015) based on data from ICESat, GRACE and modelling. The pattern found is also robust against small changes in reference elevations (such as from using the 1 arc-second SRTM DEM) or sample composition, and can also be reproduced using the most recent RGI glacier outlines — which have clearly become much more accurate since the study of Gardner et al. (2013). The regions with increasing glacier volume spatially match the areas with growing endorheic lakes on the TP and where MERRA-2 data suggests a step-like increase of summer precipitation around the year 2000. The change in available precipitation amounts, lake water volume, and glacier mass balances are of the same magnitude and match well in terms of timing. The fact that glacier volumes are predominantly increasing in regions where also lake volumes increase, and the fact that lake volumes are also increasing in little or not glacierized basins, both suggest that the increases in lake volumes over the study region are not mainly driven by increased water influx from glacier mass loss (see e.g. Song et al., 2015). Though, glacier mass loss can certainly play an additional role for lakes with declining glaciers in their catchment. This is in line with, and extents geographically, water balance modelling by Lei et al. (2013) for six selected lakes in our East TP zone (Fig. 4b) that suggests mainly precipitation increases to be behind the increases of lake volumes, accompanied by decreases in potential evaporation due to decreasing wind speed, and to a lesser extent increase in glacier runoff (Song et al., 2015). For the Siling Co lake, potential evaporation, though decreasing overall over 1961–2010, showed actually stable conditions or a slight increase between the mid/end 1990s to 2010 (Guo et al., 2019), underlining even more the key role of precipitation increases for the observed lake volume increase.

On a local scale, and in contrast to the above regional view, there are considerable differences to previous findings in glacier changes, including the ones based on the same ICESat data. Compared to a visualisation of our results in a regular grid, we find that spatial aggregation matters: even within our study, only the manual zonation brings forward finer spatial differences e.g. from topographic-orographic setting. Our results also suggest that inconsistent sampling hypsometry, snow cover, and

local vertical biases and elevation inconsistencies can have a severe biasing effect on ICESat-based glacier changes when not accounted for properly — in particular where they vary for different ICESat campaigns.

5.1 Precipitation increase on the TP

The spatial patterns of MERRA-2 decadal precipitation increases and the glacier growth on the TP and in the Kunlun Shan suggest a causal relationship. Increased precipitation in the region has been noted before: Yao et al. (2012) attributed a pattern of precipitation/glacier changes to a strengthening of the Westerlies while the Indian monsoon is weakening. Also a rise in extreme precipitation events at stations in the study region was attributed to a weakening East Asian monsoon (Sun and Zhang, 2017). Fujita and Nuimura (2011) and Sakai and Fujita (2017) model a decrease in theoretical equilibrium line altitudes (ELA) in western Tibet over 1988 and 2007, and attribute these trends to increasing precipitation in western Tibet (but decreasing precipitation in western Pamir and the western Himalaya). Several studies report that lake levels recently were increasing on the TP (e.g., Zhang et al., 2011, 2013; Song et al., 2015; Zhang et al., 2017). Glaciers in West Kunlun were in general shrinking between 1970 and 2001, only those on the south slope were already growing between 1991 and 2001 (Shangguan et al., 2007).

While the MERRA-2 data does not suggest an increase in summer precipitation in Eastern Pamir and on the western and northern boundary of the Tarim Basin, Tao et al. (2011, 2014) found indications for a wetter climate and increasing streamflow in the entire basin. Shi et al. (2007) suggest a shift from a warm-dry to a warm-wet climate in the entire northwest of China happened already around 1987. Our results suggest that glaciers on the southernmost orographic barrier in the Tien Shan are closer to balance than glaciers further north/west. We thus speculate that the change in circulation patterns behind the positive precipitation change, centred further south, extends across the entire Tarim basin, and with it more favourable conditions for glaciers on the edge of the entire basin.

Maussion et al. (2014) proposed a new classification for HMA glaciers based on their main accumulation season from 2000–2011 HAR precipitation data. Our pattern of positive glacier changes matches very well with their classification of the predominant glacier accumulation season as spring or early summer. On the TP, Maussion et al. (2014) find a gradual transition towards later accumulation (monsoon-dominated) whereas there is a crisp boundary to winter accumulation in the Karakoram/Pamir. Both patterns correspond to the zonal boundary of 'extreme continental (polar) glaciers' suggested by Shi and Liu (2000), which encompasses the northwestern half of the TP, glaciers north of central Karakoram, the easternmost Pamir, and the entire Kunlun Shan. On a coarser spatial and longer temporal scale, Kapnick et al. (2014) suggest that glacier accumulation in the Karakoram is least sensitive to atmospheric warming due to dominating non-monsoonal winter precipitation in this region.

Fujita (2008) finds that HMA's glaciers are more affected by precipitation seasonality and concentration than by changes in annual precipitation. Where accumulation and warming happen at the same time (i.e. summer), rising temperatures increase both melt and the share of precipitation that falls as rain instead of snow. While temperatures are rising in entire HMA, the glacier sensitivity study of Fujita and Nuimura (2011) suggests that temperature was not the limiting factor for glacier existence everywhere. In the extremely dry and cold TP and Kunlun Shan, with glaciers and in particular their accumulation areas at high elevations (Fig. 1), glacier growth due to increased precipitation is thus entirely plausible — despite a warming trend.

This also stresses that the altitude of HMA glaciers (Fig. 1) is an important factor in their respective responses to temperature and precipitation changes (Sakai and Fujita, 2017), and thus in the here-observed glacier volume changes.

In light of continued climatic changes in the study region, ICESat only provides a short snapshot of ongoing glacier reactions. This snapshot falls exactly into the decade where an increase in precipitation on the TP would cause the largest effects on glacier volume changes due to dynamic adjustment of the geometry in ablation areas as a delayed signal towards a new glacier equilibrium state (Kääb et al., 2018; Gilbert et al., 2018). Ke et al. (2015a) and Bao et al. (2015) report such stronger elevation gain for ablation areas compared to elevation gains in accumulation areas in what they refer to as West Kunlun Shan (our unit KS1, plus four to the North and East of it). We find the same signal for a larger area of an additional eight adjacent units, including those to the South. Care has to be taken when analysing elevation changes over only parts of a glacier as this violates the condition of mass continuity. A thickening of the ablation parts of a glacier can thus be caused by either positive surface mass balance or dynamical changes (i.e. increased ice flux). In the case of West Kunlun Shan, a stronger thickening of the tongues compared to higher elevations could indicate both were happening: a general glacier thickening from ongoing positive mass balances plus a delayed dynamical thickening from earlier mass gain in the accumulation areas. Southeast on the TP, dh–elevation gradients are largest, which could indicate that dynamical changes are happening also there: an overall thinning signal could be composed of increased melt at lower elevations, causing strongly negative dh, while the accumulation areas are growing due to increased precipitation/accumulation, causing strongly positive dh (Fig. 3d).

5.2 Glacier thinning on the Eastern Tibetan Plateau

The negative trends on the eastern border of the TP agree with reported glacier mass loss in this area, although varying annually and in space (Kang et al., 2009; Yao et al., 2012). For this part of the southeastern TP, Mölg et al. (2014) found that the competition between the monsoon and large-scale westerly waves of the mid-latitude circulation in spring/early summer determines annual mass balance. The south–north transition of the jet stream across the TP in spring varies in timing and efficiency, and its re-intensification in summer on the northern edge of the TP is related to the onset of the summer monsoon (Schiemann et al., 2009). This interplay affects both precipitation and summer air temperature. All glaciers in the region are of summer accumulation type, except for East Nyainqêntanglha Shan and Hengduan Shan (Maussion et al., 2014). The area where the atmospheric flow strength over the TP correlates strongly with summer temperatures (Mölg et al., 2014) forms an arc-shaped band from the above mentioned mountain ranges along the northern slopes of the East Nyainqêntanglha Shan to the easternmost glacierised mountains in the area. The correlation of Monsoon/Westerlies competition with temperature is decreasing rapidly north towards the easternmost Kunlun Shan and south to the Goikarla Rigyu range just north of the Yarlung Tsangpo Valley. This pattern corresponds well with our findings of only slight glacier thinning in Goikarla Rigyu/East Kunlun Shan (units N3 and KS2) but more negative volume changes in the easternmost HMA glaciers (our unit HS). Reconstructed mass balances from six glaciers on the eastern slope of Minya Gongga (in the very east of unit HS) were $-0.79\,\mathrm{m\,w.e.\,a^{-1}}$ in 2001–2009, a notable further decrease from an already negative average of $-0.35\,\mathrm{m\,w.e.\,a^{-1}}$ in 1952–2000 (Zhang et al., 2012). Converted to mass loss, our results in this area are $-0.77 \pm 0.42\,\mathrm{m\,w.e.\,a^{-1}}$ — the large uncertainty reflects the sparse

glacier coverage and low sample numbers in this unit. (Zhang et al., 2012) report that both the ELA and temperatures in the beginning and end of the melt season were strongly rising during the ICESat decade.

Glaciers in the Qilian Shan in the very northeast of the TP have been shrinking less than those further south in the last decades (Tian et al., 2014). In-situ mass balances on Qiyi glacier were strongly negative in 2005–2006 ($-0.95\,\mathrm{m\,w.e.\,a^{-1}}$) but less so in 2006–2007 ($-0.3\,\mathrm{m\,w.e.\,a^{-1}}$). The 2006 negative mass balance is indeed visible as a marked decrease between ICESat's 2005 and 2006 autumn campaign median dh in all our units north of Nyainqêntanglha Shan. We find only moderate thinning in the eastern part of Qilian Shan (converted to mass changes: $-0.26 \pm 0.14\,\mathrm{m\,w.e.\,a^{-1}}$), where Qiyi Glacier lies, and even less negative values further west ($-0.14 \pm 0.10\,\mathrm{m\,w.e.\,a^{-1}}$), in line with Tian et al. (2014). Towards east, glaciers become smaller and elevations lower, and the influence of the East Asian Monsoon becomes stronger.

5.3 Glacier sensitivity to precipitation in the Himalaya

We find consistently less negative glacier volume changes on the first orographic ridge across the entire Himalayan Range. Misclassifications of e.g. perennial snow patches with stable surface elevations classified as glaciers would cause a mixed glacier/land trend with a weaker surface lowering signal. To achieve this effect, the misclassification would have to be severe (ca. half of the samples) and be present in both our manual classification and the RGI, as the pattern is visible with both glacier classifications. We carefully classify our samples manually to avoid precisely such mixed signals, thus we consider this bias unlikely. Another cause could be reduced melt due to insulation from debris cover. It has previously been shown that stagnant (debris-covered) tongues lose mass at a similar rate as clean ice glaciers (Kääb et al., 2012; Gardelle et al., 2012b; Pellicciotti et al., 2015; Ragettli et al., 2016). We thus assume that debris-cover is not the cause of the observed differences.

Locally varying sensitivity to precipitation might also explain the less negative mass balances on the first, and thus wettest, orographic ridge in the Himalaya. Precipitation from summer monsoon influx decreases sharply after large changes in relief (Bookhagen and Burbank, 2006). Maussion et al. (2014) find that precipitation regimes are strongly varying over short distances in the Himalaya, not least due to glacier orientation on the windward or lee side of the a mountain range. Wagnon et al. (2013) and Sherpa et al. (2016) mention the meteorologically exposed location of Mera glacier (4949–6420 m a.s.l.) in the Khumbu region, Nepal, as a possible explanation of its roughly stable mass balance since 2007 when in-situ measurements began. This stands in stark contrast to the considerable mass loss seen in Pokalde and Changri Nup glaciers only 30 km further north (the latter are also smaller and located at lower and thus warmer elevations, which likely contributes to these differences). In our ICESat zonation, these glaciers are located in units H1 ($-0.12 \pm 0.25\,\mathrm{m\,a^{-1}}$) and H2 ($-0.50 \pm 0.32\,\mathrm{m\,a^{-1}}$). Wagnon et al. (2013) note that in the DEM differencing study of Gardelle et al. (2013), larger glaciers in the same range as Pokalde/Changri Nup also seem to experience more surface lowering than Mera glacier further south.

Our consistently less negative glacier volume changes of the first orographic ridge across the entire Himalayan Range supports the interpretation of Wagnon et al. (2013) and Sherpa et al. (2016), and suggests the effect is visible along the entire Himalayan Range. However, the 2004–2008 average annual mass balances of the well-studied Chorabari and Chhota Shigri glaciers in western Himalaya do not follow this pattern. South-facing Chorobari lies on the outermost orographic ridge and lost mass at a rate of -0.73 metres water equivalent per year ($\mathrm{m\,w.e.\,a^{-1}}$, Dobhal et al., 2013), which is comparable to

north-facing Chhota Shigri's balance of -0.9 m w.e. a^{-1} (Ramanathan, 2011). Both glaciers lie at comparable elevations (ca. 4000–6400 m a.s.l.).

The ELA sensitivity study of Fujita and Nuimura (2011) is too coarse to confirm orography-related spatial differences across the Himalaya, but along the mountain ridge their findings correlate well with both Yao et al. (2012) and our pattern of glacier changes in the inner Himalayan ranges (Sakai and Fujita, 2017, see also). In particular the stable glacier elevations in our unit HK1 — between areas of glacier loss in the Hindu Kush and the particularly negative western Himalaya (units H4–H6) — are backed up by their modelled stable ELAs. The particularly negative surface elevation change in the western Himalaya has previously been attributed to rapidly shrinking accumulation areas, seen in rising firn lines in Landsat images (Kääb et al., 2015, area called Spiti Lahaul). Kääb et al. (2015) see the same pattern for the strongly negative glacier evolution in Nyainqêntanglha Shan/Hengduan, which has low-lying accumulation areas. Thus, once the accumulation area becomes too small or disappears entirely, also abundant or increasing precipitation cannot compensate for melt due to increased temperatures (Sakai and Fujita, 2017).

5.4 Dissimilar glacier behaviour in the Karakoram/Kunlun Shan

The zonation we present here is the result of an compromise between within-unit glacier similarity, representative sampling, and stable glacier surface change trends. In the Karakoram/Kunlun Shan area, this approach is clearly more appropriate than sample grouping into a regular grid. The latter results in large trend uncertainties (Fig. 2b), since grid cells include both the thinning signal south of the central Karakoram and thickening signal in the Kunlun Shan.

In the Karakoram, we see indications of surging glaciers/glaciers recovering from a surge. In most units, such as K1–K3, the surface elevation change signal is different in the upper 50% elevations compared to the ablation areas. This is in line with e.g. Gardelle et al. (2013) or Gardelle et al. (2012a), who find that most of the glaciers in this area were in some stage of a surging cycle in the ICESat decade. Our units are just large enough not to be dominated entirely by a retreating or rapidly growing tongue of one single large glacier, but rather provide an average of these locally different signals. After ensuring correct hypsometry sampling, the surface elevation changes of the different units in the area agree well. We find evidence of surging glaciers also in other areas, such as the Zhongfeng glacier in the Western Kunlun Shan (unit KS1) (Ke et al., 2015a). ICESat does not sample the tongue of Zhongfeng glacier (whose surface might be rising) and the negative elevation trend dominates the signal in the unit — which does not fit the otherwise positive elevation change of the surrounding units. Aggregated in larger spatial units such as a regular grid, this local peculiarity is not visible. Whether such signal is representative for all glaciers in a unit or not would require complete geodetic analysis of all glaciers and also a longer time span.

5.5 Varied pattern in Tien Shan

Glacier evolution in the Tien Shan has shown a spatially diverse pattern already in the last decades of the 20th century (Narama et al., 2010; Farinotti et al., 2015). Together with contributions from northerly areas, the Westerlies are the source of precipitation for the entire region (Bothe et al., 2012), but there are different climatic sub-regions: glaciers in the Western Tien Shan (and Pamir Alai) receive precipitation mainly in winter, the northern and northeastern ranges both in winter and summer, whereas

the inner ranges are of the spring/summer accumulation type (Sorg et al., 2012). In the (north)western Tien Shan, our zonation does not consider this transition from winter-only to summer/winter precipitation. The thinning rate in this unit is dominated by glaciers in the eastern part (two thirds of all samples are in Ile and Kungoy Alatau). Between 1961 and 2012, Farinotti et al. (2015, modelled balances) found that glaciers in the very west (Pskem) lost more mass than those further east (Ile and Kungoy Alatau). Farinotti et al. (2015) also used ICESat, but their 2003–2008 results for Ile and Kungoy Alatau are more negative (-0.68 ± 0.44 m w.e. a^{-1}, at 2σ) than both their modelled mass balances for the same area (-0.33 ± 0.16 m w.e. a^{-1}) and our result for the entire western Tien Shan. Splitting the unit, our ICESat data indeed shows stronger glacier thinning west of Issyk-Kul but only with high uncertainty, caused by spatially strongly varying vertical offsets (or very varied glacier behaviour) which clearly add temporal variability to campaign median dh.

Narama et al. (2010) suggest that glaciers of the outer ranges, which receive more precipitation are melting faster since they have a higher mass turnover and their tongues are at lower elevations. They see such a pattern in 2000–2007 glacier shrinkage, which was more pronounced in the Western/northern Tien Shan than in interior areas such as the southeastern Fergana Range or At-Bashy Range at the transition to the Pamir. Our thinning rates do not confirm this — precisely in this latter area (unit P3), we find the most negative glacier surface elevation changes in the entire region (converted to mass change: -1.04 ± 0.23 m w.e.). However, the modelling study of Farinotti et al. (2015) suggests spatially highly varying glacier reactions in the last few decades in that area (their coarser zonation in the Central Tien Shan does not allow direct numerical comparison with our results).

In the inner Tien Shan, our elevation change rates vary on a small spatial scale. To some degree, the pattern resembles the land trends which indicate an influence of spatially varying elevation bias or snow cover in December 2008. Subtracting the negative land trends from the glacier trends greatly reduces the local differences. Reconstructed annual mass balances of Batysh Sook glacier and glacier No. 354 were -0.37 and -0.47 m w.e. a^{-1} respectively (average 2003–2008; Kenzhebaev et al., 2017; Kronenberg et al., 2016), and also DEM differencing/modelling studies in the area found similar values (Fujita and Nuimura, 2011; Shangguan et al., 2015; Barandun et al., 2018). Our zonation does not consider glacier aspects, which seem to play an important role in explaining glacier melt over this region (Farinotti et al., 2015).

For the glaciers in the Aksu-Tarim catchment in central Tien Shan, Pieczonka et al. (2013) found a decelerated mass loss between 1999 and 2009 (-0.23 ± 0.19 m w.e. a^{-1}) compared to earlier decades, which supports our only slight thinning on the northern slopes of the Tarim basin. Our units with less thinning resemble the pattern of glaciers with little long-term changes by Farinotti et al. (2015, modelled) — except for our balanced glacier signal in the southern Halik Shan on the northeastern edge of the Tarim basin. The few glaciers in this unit are small and lie at lower elevations, which would make them prone to fast melting in a warming climate. This is what Farinotti et al. (2015) found for the entire Halik Shan (2003–2009: -0.69 ± 0.28 m w.e. a^{-1} modelled, -0.68 ± 0.43 ICESat) and corresponds to our thinning rates in the northern parts of the Halik Shan.

ICESat suggests more moderate thinning for the north-eastern Borohoro range (converted: -0.44 ± 0.22 m w.e. a^{-1}), and even less negative values for the glaciers in the central Borohoro range (TS1, converted: -0.09 ± 0.18 m w.e. a^{-1}) that are at higher elevations. Farinotti et al. (2015) found that the central parts of the range receive 50% more summer precipitation compared to the rest of the range, and modelled -0.17 ± 0.24 m w.e. a^{-1} for 2003–2009 for a slightly larger area than our most central unit. There, our thinning rates fit better to their modelled glacier balances than their ICESat-based mass loss estimates.

The Cryosphere Discuss., https://doi.org/10.5194/tc-2018-238
Manuscript under review for journal The Cryosphere
Discussion started: 12 November 2018

The opposite is the case for the northernmost range (Djungar Alatau), where both our (converted: -0.81 ± 0.16 m w.e. a^{-1}) and their ICESat-based results (-0.75 ± 0.52 m w.e. a^{-1}) are nearly twice as negative as their modelled average 2003–2009 mass balances.

A method discussion, in particular on biasing influences on ICESat glacier surface elevation change rates is provided in Appendix D.

6 Conclusions

We present the first complete, spatially resolved and consistent estimate of glacier volume changes in entire High Mountain Asia (HMA) for 2003–2008 based on ICESat data. The study confirms existing knowledge about glacier change in the region, but also addresses several new aspects and stresses in particular the role of precipitation and elevation sensitivity of glaciers in different parts of HMA. To confirm underlying precipitation changes on the Tibetan Plateau (TP) with an independent approach, we estimate the 1990–2015 change in total water volume from all endorheic lakes on the TP, based on variations in both areal extent and water surface levels. The latter work results in volume change time series of >1300 lakes, much more than available so far. In more detail, we conclude:

- Only carefully delineated spatial units show local patterns of glacier change that are diluted or hidden if samples are gridded. On a larger scale, the pattern we find in this study agrees with previous regional estimates based on ICESat — but provides finer detail.
- The pattern of glacier changes is spatially very varied because glacier elevations, and their sensitivity to temperature and precipitation changes vary spatially (Sakai and Fujita, 2017; Kapnick et al., 2014). Together with glacier elevations, precipitation distribution and changes are able to explain large parts of the general glacier change pattern observed for 2003–2008.
- An almost step-like precipitation increase on the TP, Kunlun Shan and possibly also the Tarim Basin between 1995 and 2000 is clearly visible from changes in lake water volume as well as MERRA-2 reanalysis data. The precipitation increase is able to fully explain 2003–2008 glacier thickening in an area centred over the Kunlun Shan. The boundary between positive and negative glacier changes is sharp in the Kunlun Shan and formed by the Muji Basin, upper Gez river and Tashkurgan Valley. It is more gradual on the TP.
- Lake volume changes on the TP reflect a clear and comparably sudden increase of water availability from 1997 through ~2010 for the northern and eastern TP, but only minor changes in the southwestern TP and Qilian Shan. The observed lake changes correspond to a precipitation-equivalent 6–7 mm a^{-1} for the northern TP and 25 mm a^{-1} for the eastern TP, from decadal averages between the 1990s and 2000s. According to MERRA-2 reanalysis data, the change can exclusively be driven by increased summer precipitation of 34–100 mm decadal difference between the 1990s and 2000s. Decreasing potential evaporation from reduced wind speeds is also suggested to have in general contributed to lake growth (with uncertain timing though). Only in some areas increased influx from glacier mass loss should have contributed to

lake growth as the zone of lake growths roughly coincides with the zone of positive glacier mass balances. The magnitude of lake volume change, glacier mass balance and precipitation changes agree within each other, considering also evaporation.

- Glaciers on the TP changed their geometry during 2003–2008. In the northeastern TP/western Kunlun Shan, upper glacier surface elevations were stable while tongues were growing. Further south/east, upper elevations were thickening while the tongues were thinning due to both increased accumulation and melt. The further southeast on the TP, the stronger the glacier thinning rates. Glaciers in the Qilian Shan were only moderatly losing mass.

- Along the entire Himalayan Range, glaciers on the first orographic ridge were thinning less than those further back in a drier climate, likely due to abundant precipitation on the first ridge, which causes ELAs to be at lower elevations. Precipitation and ELA gradients might be very steep in the outermost ridges of the Himalaya.

- Glaciers in the Tien Shan were thinning rather more than in other parts of HMA, in particular those in the transition between the Tien Shan and Pamir mountains. There are exceptions to this general trend: glaciers in the central Borohoro range (at higher elevations) and on the northern slopes of the Tarim Basin were close to balance, possibly due to precipitation increase.

- From a methodological point of view, this work stretches the applicability and precision of ICESat-derived elevation changes in rough and glacierised terrain further than was the case for previous studies. We carefully examined the influence of how spatial units are delineated to derive ICESat-based glacier change over HMA as well as a range of potential biases and error influences on the analyses.

While the glacier change pattern presented in this study is robust and well explained by glacier sensitivities to climate change, our unit boundaries might not match areas of consistent glacier changes everywhere, despite best efforts. Low ICESat sample density prohibits a further refinement in areas with sparse glacier coverage. Other remote sensing data with finer spatial resolution could improve the pattern — for example DEM differencing from ASTER stereo-imagery (Brun et al., 2017) and other spatially extensive data available for the last decades, or also ICESat-2, once this data becomes available.

Code and data availability. ICESat data are freely available from NSIDC and NASA, the SRTM DEM and Landsat data from USGS, the MERRA-2 reanalysis data from NASA Goddard Earth Sciences Data and Information Services Center, ERA Interim from the European Centre for Medium-Range Weather Forecasts, the Global Surface Water dataset within Google Earth Engine. The derived ICESat zonation is available from the authors upon request.

The Cryosphere Discuss., https://doi.org/10.5194/tc-2018-238
Manuscript under review for journal The Cryosphere
Discussion started: 12 November 2018

Appendix A: Data

A1 ICESat elevation data

The NASA Ice, Cloud and land Elevation Satellite (ICESat) measured the Earth's surface elevations in two to three campaigns per year from 2003 to 2009. The campaigns were flown in northern autumn (∼ October–November), winter (∼ March), and early summer (∼ June). Autumn is overall the driest season in HMA, and ICESat's autumn elevation samples on glaciers thus fall to a large extent on ice and firn rather than fresh snow. By contrast, snow falls in March/June in parts of HMA. ICESat's Geoscience Laser Altimeter System (GLAS) sampled surface elevations within ground footprints of ∼ 70 m in diameter (Schutz et al., 2005). Elevation samples are separated by ∼ 170 m along ground tracks/orbits but up to 75 km between orbit paths in HMA. The ground track pattern was not repeated exactly during each overpass, as the near-repeat orbit mode was not activated at lower latitudes (Schutz et al., 2005). Rather, individual ground tracks lie as far as 2–3 km from the reference ground track in HMA. A direct comparison between ICESat elevations is thus difficult in the region. Instead, double-differencing techniques are applied, i.e. comparing ICESat elevations with a reference DEM to receive elevation differences and analysing their subsequent evolution over time (Kääb et al., 2012; Gardner et al., 2013; Neckel et al., 2014; Kääb et al., 2015; Ke et al., 2015a).

Here, we use GLAS/ICESat L2 Global Land Surface Altimetry HDF5 data (GLAH14, release 34) which is optimised for land surfaces (Zwally et al., 2012). From comparison with reference DEMs, elevation uncertainty of GLAH14 data was found to be on the order of decimetres to metres in mountainous terrain in Norway (Treichler and Kääb, 2016). Elevation biases and inconsistencies throughout ICESat's lifetime are of centimetre to decimetre magnitude and thus negligible compared to uncertainties from the underlying terrain and biases in the reference DEM (Kääb et al., 2012; Treichler and Kääb, 2016).

A2 SRTM DEM

The DEM from the Shuttle Radar Topography Mission (SRTM, Farr et al., 2007; Farr and Kobrick, 2000) is a consistent DEM in the HMA region. We used the C-band, non-void-filled SRTM DEM version at 3 arc-seconds resolution (SRTM3, corresponding to 92 m in y, and 66–82 m in x-direction at 45/28° N) which is accessible from the U.S. Geological Survey at https://dds.cr.usgs.gov/srtm. The SRTM DEM used here is a product of single-pass C-band SAR interferometry from images acquired on 11–22 February 2000 (Farr and Kobrick, 2000). SRTM DEM nominal vertical accuracy is of the order of metres (Rodriguez et al., 2006). Treichler and Kääb (2016) found spatially varying vertical offsets on the order of metres to decimetres in mountainous terrain in Norway. They attributed the vertical biases to the fact that the SRTM DEM is a composite from several individual images and overpasses, and likely processed in (unknown) spatial sub-units. Offsets caused by shifts of sub-units were not removed by global DEM co-registration, but the bias/uncertainties caused by them are within the nominally stated accuracy. On glaciers, larger elevation uncertainties are to be expected due to penetration of the C-band signal into ice and, even more so, into snow. Also dry sedimentary soils may be subject to radar penetration. The penetration is estimated to be in the range of several metres for glaciers in HMA (Gardelle et al., 2012a; Kääb et al., 2012, 2015).

The vertical offsets from DEM shifts or penetration increase the uncertainty of surface elevation changes — possibly also for ICESat-based studies, if the spatial pattern of SRTM DEM offsets interferes with ICESat's spatial sampling pattern (Treichler

and Kääb, 2016, 2017). As an alternative elevation reference, we used the SRTM DEM at 1-arc-second resolution (SRTM1) from https://earthexplorer.usgs.gov. The 1-arc-second DEM has undergone fewer revisions than the 3-arc-second DEM, making the data not necessarily superior, and most data voids are filled in with other elevation data that have different time stamps. We therefore excluded the data void areas contained in the 3-arc-second DEM version also in the SRTM1 DEM to ensure that we only use original elevation data from February 2000. Further, we did not explore or use the recently published TanDEM-X global DEM as it was not available during our processing. It remains to be investigated how potential advantages of this DEM (larger coverage, less penetration than C-band) balance potential disadvantages (longer time difference to ICEat period, temporal inconsistency from stacking). Also due to temporal inconsistency and substantial voids, we did not use the ALOS PRISM World DEM (AW3D) or the WorldView satellite optical stereo HMA DEM.

A3 Precipitation data

As an estimate for regional and temporal precipitation patterns for the years 1980–2015 we use data from the Modern-Era Retrospective analysis for Research and Applications, version 2 (MERRA-2 Bosilovich et al., 2016) at resolution of 0.625° x 0.5° in lat/lon and available from the NASA Goddard Earth Sciences Data and Information Services Center at https://disc.sci.gsfc.nasa.gov/mdisc, and ERA Interim (Berrisford et al., 2011) at T255 spectral resolution (0.7° lat/lon), available from the European Centre for Medium-Range Weather Forecasts at http://apps.ecmwf.int/datasets/. We use monthly summarised values of the variables total precipitation (PRECTOT / tp), snowfall (PRECSNO / sf) and evaporation (EVAP / e) from MERRA-2's surface flux diagnostics dataset tavg1_2d_flx_Nx (GMAO, 2016) and ERA Interim's Monthly Means of Daily Forecast Accumulations, respectively. The High Asia Reanalysis (HAR, Maussion et al., 2014), a product optimised for the TP region and with much finer spatial resolution, is unfortunately only available for the time period 2001–2011 which is too short for our study with respect to the lake volume changes investigated.

Further, we use in-situ data from the five westernmost meteorological stations on the TP and Kunlun Shan (Fig. 1), provided by the China Meteorological Science Data Sharing Service Network. The stations are located relatively close to the area with reported glacier mass gain (we are not aware of any meteorological measurements on the northeastern TP). The data includes daily measurements of precipitation, mean air temperature, and for the four stations on the southwestern TP also evaporation.

A4 Global Surface Water Dataset

The Global Surface Water dataset (Pekel et al., 2016) is a classification of the entire Landsat archive into monthly and annual maps of surface water (https://global-surface-water.appspot.com). The data is available within Google Earth Engine (Gorelick et al., 2017). To map the changing extents of Tibetan lakes, we used the variable occurrence which provides the classes no data, no water, water (for both monthly/annual data), and seasonal water (for annual maps only). Coverage is nearly complete (>98%) starting from 2000 but considerably worse for some years of the 90s (Pekel et al., 2016, for our areas of interest: 20–75% no data pixels in 1990, 1991, 1995, 1997 and 1998).

The Cryosphere Discuss., https://doi.org/10.5194/tc-2018-238
Manuscript under review for journal The Cryosphere
Discussion started: 12 November 2018

Appendix B: Methods for glacier volume change

We follow the double-differencing method explained in further detail in Kääb et al. (2012) and Treichler and Kääb (2016), with special consideration of issues mentioned in the above introduction. ICESat data and individual SRTM DEM tiles were converted into the same geographical reference system, co-registered (Nuth and Kääb, 2011), and reference elevations for ICESat footprint centres retrieved by bilinear interpolation. The difference between ICESat and SRTM elevations is further referred to as dh. Double differencing, i.e. fitting a linear trend through dh from several years, reveals how much the surface elevation has changed on average over the time period studied.

ICESat samples were reduced to those within a 20 km buffer around RGI glacier outlines. To avoid inclusion of off-glacier elevation samples in our glacier surface change analyses (see introduction), we classified all ICESat footprints manually into *ice* and *land* samples, using the most snow-free Landsat images from ca. 2000–2013. Samples on water and clouds ($|\mathrm{dh}| > 100$ m) were excluded. Samples on glacier borders were also excluded, to avoid inclusion of 70 m footprints that only partially fall on ice and because glacier areas could have changed in the course of 2003–2008 (Treichler and Kääb, 2016). We used only samples from ICESat's 2003–2008 autumn campaigns to avoid bias from temporal variations in snow depths (see introduction). After filtering, 74'938 ice samples and about ten times as many land samples remain. To compute statistics per glacier, we also classified the samples based on glacier outlines of the newest version of the RGI (version 5, Arendt et al., 2015).

Per spatial unit, we estimate glacier surface elevation change by fitting a robust linear regression (which minimizes an iteratively weighted sum of squares) through individual dh (Kääb et al., 2012). To test the sensitivity of biased dh at either end of the studied time period, we also compute a t-fit (Treichler and Kääb, 2016) and a non-parametric Theil-Sen linear regression (Theil, 1950; Sen, 1968). Both alternative robust fitting algorithms better fit our dh distribution and are commonly used for datasets with large natural variability and measurement errors. Our final estimate per spatial unit corresponds to the average of the three trend methods.

B1 Zonation

ICESat data needs to be grouped into spatial units to fit surface elevation trends. The samples within each spatial unit need to reflect the glaciers in a representative way. This condition is easier to fulfil if the glaciers are similar to each other, including their 2003–2008 mass balances and their variations. We tested automated clustering methods from ICESat dh directly, but were not successful. We therefore preferred to delineate spatial units manually, considering topographic and climatic setting, elevation, visual glacier appearance, and input from literature and discussions with experts. In particular, we paid attention to orographic barriers. The zonation we present here is thus the result of an iterative manual process of re-defining spatial units until they yielded statistically stable and robust glacier surface change estimates. While the procedure is based on carefully applied expert knowledge, we are fully aware that our zonation is eventually a subjective one and certainly open to discussion. As a control approach, we applied the same gridding method as Kääb et al. (2012, 2015) to the entire HMA.

B2 Glacier hypsometry

We compute the relationship between glacier dh and elevation (hereafter called dh–elevation gradient) by fitting a robust linear regression through individual glacier samples' dh vs. elevation. Greater radar penetration in the accumulation areas and more prominent melting of tongues steepen dh–elevation gradients (e.g. Vijay and Braun, 2016; Ragettli et al., 2016). It is therefore very important to ensure ICESat's elevation sampling is consistent through time and representative for glacier hypsometry (see introduction). Our primary approach to improve sampling hypsometry is to enlarge spatial units, but in some areas this would have in turn led to considerably reduced glacier similarity within the unit. To account for these conflicting cases, we computed four different corrections and compared the such-adjusted results: (A) correcting the slope of the glacier elevation-change trend for the effect of a positive/negative elevation trend in time; (B) correcting individual dh for the effect of elevation, i.e. computing the expected dh from the dh–elevation gradient and the individual elevations sampled, and removing the expected dh values from the measured dh values; (C) filtering of the samples of each ICESat campaign to match the hypsometry of the glaciers within each spatial analysis unit; (D) assigning weights to samples depending on their elevation so that they match the glacier hypsometry, i.e. analogue to C but without removing any samples.

Methods A and B are based on the method used in Kääb et al. (2012, 2015). If ICESat consistently samples lower (or higher) elevations than the reference hypsometry, methods A and B will not correct for this — they only correct elevation-induced bias relative to the mean sampled elevations of all campaigns. Methods C and D, however, adjust the hypsometry so that it should become representative for the glacier elevations in the unit. All four corrections are here applied to all units, and both for ice and land samples separately. Our 'standard method' for the final glacier elevation change estimates corresponds to the average of all hypsometry-correcting methods (A–D) and trend methods (robust, t- and Theil-Sen trends). Additionally, we also compute trends for only the upper/lower 50% glacier elevations as from RGI hypsometries (samples above/below the median RGI glacier elevation in each unit). The latter analysis violates mass conservation and should thus not be interpreted in terms of mass balance, but rather, for instance, for changes in glacier elevation gradients (e.g. Brun et al., 2017; Kääb et al., 2018).

B3 Correction of vertical bias

Glacier elevation difference dh may be subject of vertical bias originating from local reference elevation bias or snow fall during the second part of the autumn 2008 campaign. Local vertical bias may result from inconsistent reference DEM age or production, tiling and tile/scene misregistration, or locally varying radar penetration (in case of the SRTM DEM). To remove this bias, we compute a per-glacier elevation correction cG corresponding to the median dh for each glacier, according to the method described in Treichler and Kääb (2016). In that study, the correction successfully reconciled annual ICESat-based glacier elevation changes with mass balance time series from in-situ measurements. Also in the present study, cG-corrected dh (in combination with above hypsometry methods A–D) remove the effect of a varying spatial composition of elevation offsets. However, as the correction results in lower sample numbers and removes parts of the signal where some glaciers are only sampled in the beginning and some other glaciers only in the end of the ICESat acquisition period, the correction shows

a tendency to erroneously flatten out linear trends. We thus only apply cG to 6 units, where the opposite is the case and trends from become steeper after cG correction.

Treichler and Kääb (2016, 2017) found that ICESat clearly records the onset of winter snowfall in Norway during the split autumn 2008 campaign (stopped half way in mid-October and completed only in December). This could be the case for parts of HMA, too — in particular in areas under influence by the Westerlies (Tien Shan, Pamir, Karakoram, western Himalaya) or winter precipitation in Nyainqêntanglha Shan/Hengduan Shan (Maussion et al., 2014). Analogue to Treichler and Kääb (2016), we estimate December 2008 snow bias from a linear regression of October/December 2008 land dh on elevation and time. The correction is computed individually for each spatial unit.

Appendix C: Methods for lake volume change

We compute annual water volume change of the Tibetan lakes by multiplying annual lake areas with water level changes from repeat water surface elevations for each year over the period 1990–2015. Maximum annual lake extents are obtained directly from the Global Surface Water data set by exporting bitmaps of annual water occurrence over the entire TP, using the web API of Google Earth Engine. The data is exported at a resolution of 50 m $\times$ 38–44 m in lat/lon (corresponding to 0.00045 degrees). Subsequently, we retrieve the corresponding lake surface elevations in two ways: a) from SRTM DEM elevations of the lake shore by computing the median of interpolated DEM elevations for lake shore cells for each areal extent, and b) directly from ICESat footprint elevations on the lake areas for those lakes where ICESat data is available. To extend the lake elevation time series from method b) beyond the ICESat period of 2003–2009, we compute the area–surface-elevation relationship for each lake by robust linear regression and apply this function to the areal extends of the years before and after the ICESat period. We extract the relationship both for annual time series and individual ICESat campaigns (2–3 campaigns each year, using the monthly water classifications). The so-extrapolated surface elevation values generate complete 1990–2015 time series for both areal extent and lake levels from SRTM and ICESat data, respectively. Our method is in parts similar to the methods used by previous studies investigating lake volume changes on the TP from satellite data (Zhang et al., 2011; Kropáček et al., 2012; Song et al., 2013; Zhang et al., 2013; Song et al., 2015; Zhang et al., 2017, e.g.,) but the inclusion of a DEM for deriving shoreline elevations, and thus lake water levels, in addition to altimetry data enabled us to produce volume change time series for one order of magnitude more lakes than derived previously.

We apply our procedure to the 1364 endorheic lakes on the TP and in the Qaidam Basin (Fig. 1) with a maximum lake extent of $> 1\,\mathrm{km}^2$. We generated here our own lake database since we found that existing collections, such as the Global Lakes and Wetlands Database (Lehner and Döll, 2004), are lacking numerous lakes that likely only emerged during the last two decades. Consulting satellite imagery like Landsat data, we manually adjusted our lake database to remove delta-like seasonal wetlands from water inflow on sloping terrain from the lake masks, we excluded non-endorheic lakes (visible outflow), and we excluded inundated areas affected by human interventions (e.g. for salt production) (133 wetlands not included in the above number).

The Cryosphere Discuss., https://doi.org/10.5194/tc-2018-238
Manuscript under review for journal The Cryosphere
Discussion started: 12 November 2018

C1 Uncertainties and filtering

To minimise the effect of uncertainties in or erroneous estimates for individual years, we analyse time series in a summarised way through regression over time and as decadal averages. Uncertainties associated with the lake data used include misclassification of water area in the Global Surface Water dataset (Pekel et al., 2016), lake surface elevation errors and local bias in the SRTM DEM, and bias in ICESat surface elevation measurements. For each lake and year, we compute the percentage of missing data (e.g. from cloud cover or classification voids), and years with $< 95\%$ of data coverage within the lake masks are excluded from further analyses. Lake time series that, after removing these years of insufficient coverage, do not contain any data from the 1990s are excluded entirely. For ICESat-derived lake levels, only lakes with measurements from at least three laser footprints each from at least five years are considered. Despite the lake areas and surroundings being extremely flat, SRTM DEM cells indicate up to 10 m elevation differences between neighbouring cells in a seemingly random way, and the SRTM DEM turns out to be the dataset within our lake change analysis with the greatest uncertainties. For some lakes, SRTM DEM errors result even in negative area–lake-surface elevation relationships, i.e. lake shore elevations seemingly decrease for expanding lake areas which is physically not plausible. We therefore excluded all lakes with either a negative area–lake-elevation relationship or where the 26-year linear trends for lake area and lake surface level do not have the same sign. This is done both for ICESat- and SRTM-derived lake level estimates. The overall error for a decadal average lake volume stage is estimated as the error of the mean, and for decadal differences propagated as the root of the sum of squares of the two errors (RSS).

C2 Endorheic basins

To estimate the lake water volume change in a way that can be related to glacier mass balances and precipitation changes (i.e. mm w.e. per m^2), we summarise and spatially distribute the water volume changes of all lakes within spatially confined basins. These basins are based on endorheic catchments, but because many catchments only contain a single lake and exact catchment areas are not well defined on the TP (e.g., in very flat areas), we manually controlled, adjusted and aggregated the endorheic catchments of the USGS HydroSHEDS dataset at 15 arcsec spatial resolution (Lehner and Döll, 2004, https://hydrosheds.cr.usgs.gov) to larger basins of comparable size and consisting of in average 5 catchments. We define the total lake area per catchment (and basins) as the sum of the 1990–2015 median lake area of all lakes within the spatial unit, also including the endorheic inundated areas confined by human infrastructure mentioned above, which are otherwise excluded from analyses. To compute total water volume change per catchment, we assume that lakes excluded from the analysis (see previous subsections) behaved the same way as the average of the lakes we have sufficient data for, and subsequently scale the total volume change accordingly. For total water volume change from decadal averages, we compute the error as the sum of the errors of all individual lakes' volume change (see above), again scaled according to the share of total lake area we have sufficient data for. This conservative approach of adding errors (instead of root-sum-of-squares, RSS, for instance) includes as a worst case the full correlation of the behaviour of all contributing lakes.

The Cryosphere Discuss., https://doi.org/10.5194/tc-2018-238
Manuscript under review for journal The Cryosphere
Discussion started: 12 November 2018

Appendix D: Discussion of biasing influences on ICESat glacier surface elevation change

Representativeness of samples within spatial units is the key requirement for robust glacier thickening/thinning estimates. However, we found that enlarging spatial units was not always the best remedy to ensure sample representativeness: In some areas this would have considerably reduced glacier similarity within the unit. Applying a regular grid can have this same effect. Consequently, only carefully adapted zones can show local peculiarities that are otherwise diluted.

Especially for small units with few samples, careful consideration of how potentially biasing factors interplay is important. Our use of four different methods to ensure correct hypsometry sampling makes the results very robust. The overall pattern is not affected by zonation, small changes in sample composition (RGI outlines), or reference DEM (here: SRTM1). Of all corrections, the most essential requirement is therefore that the regional glacier hypsometry is sampled appropriately, also over time. Locally, however, the different methods and corrections can result in considerable differences between glacier thickening/thinning rates. Especially where ICESat data is used on a local scale or as input for modelling studies, we strongly recommend to carefully assess the difference between hypsometry corrections, the effect of our per-glacier correction cG, and the influence of snow cover, in order to ensure a representative estimate and appropriate uncertainty.

Our snow correction affects trends significantly. In southern Norway, the study region for which the correction was developed, it removed a positive land trend but did not affect the glacier trend (Treichler and Kääb, 2016). Our results in HMA show that trend fitting methods are surprisingly sensitive to a lowering of the last (half) campaign, no matter which trend fitting algorithm is used, and for both land and glacier dh. In contrast, if the same correction is applied to a campaign between 2004 and 2007, trends only change marginally. Due to too few land samples in either of the autumn 2008 campaigns, we did not succeed to compute a correction for all units which makes the approach inconsistent, and we therefore decided not to include the correction in our final trend estimate. However, the exercise shows that November/December 2008 snow fall has the potential to erroneously decrease ICESat-derived glacier thinning rates, in particular in Tien Shan, Pamir, Hindu Kush, Nyainqêntanglha Shan/Hengduan Shan and maybe also the outer Himalayan ridges. We therefore recommend to assess the bias potential of December 2008/October snow fall for ICESat studies on a smaller spatial scale. Also, we advise not to rely on ICESat's March campaigns for glacier studies wherever snow is falling in winter in the northern hemisphere.

ICESat elevations have previously been used to estimate SRTM penetration (Kääb et al., 2012, 2015; Shangguan et al., 2015). On glaciers where no ICESat data is available, dh–elevation gradients of larger spatial units — such as in this study — could improve the estimated elevation dependency of penetration.

Author contributions. D. Treichler jointly designed the study with A. Kääb, performed all data analyses and prepared the manuscript. A. Kääb contributed to data interpretation and edited the manuscript. N. Salzmann and Ch.-Y. Chu contributed to analyses and interpretation of the climate/precipitation signals and lake water volumes, and the joint interpretation of the data.

Competing interests. The authors declare no competing interests.

Acknowledgements. The study was funded by the European Research Council under the European Union's Seventh Framework Programme (FP/2007-2013)/ERC grant agreement no. 320816, the ESA project Glaciers_cci (4000109873/14/I-NB) and the Department of Geosciences, University of Oslo. We are very grateful to NASA and USGS for free provision of the ICESat data and the SRTM DEM version we used, respectively. Special thanks go to Patrick Wagnon, Joe Shea and the Cryosphere group at ICIMOD, Nepal, and Martin Hölzle, Martina Barandun and the Physical Geography group at the University of Fribourg, Switzerland, for their valuable input on the spatial zonation.

References

Arendt, A., Bliss, A., Bolch, T., Cogley, J., Gardner, A., Hagen, J.-O., Hock, R., Huss, M., Kaser, G., Kienholz, C., Pfeffer, W., Moholdt, G., Paul, F., Radić, V., Andreassen, L., Bajracharya, S., Barrand, N., Beedle, M., Berthier, E., Bhambri, R., Brown, I., Burgess, E., Burgess, D., Cawkwell, F., Chinn, T., Copland, L., Davies, B., Angelis, H. D., Dolgova, E., Earl, L., Filbert, K., Forester, R., Fountain, A., Frey, H., Giffen, B., Glasser, N., Guo, W., Gurney, S., Hagg, W., Hall, D., Haritashya, U., Hartmann, G., Helm, C., Herreid, S., Howat, I., Kapustin, G., Khromova, T., König, M., Kohler, J., Kriegel, D., Kutuzov, S., Lavrentiev, I., LeBris, R., Liu, S., Lund, J., Manley, W., Marti, R., Mayer, C., Miles, E., Li, X., Menounos, B., Mercer, A., Mölg, N., Mool, P., Nosenko, G., Negrete, A., Nuimura, T., Nuth, C., Pettersson, R., Racoviteanu, A., Ranzi, R., Rastner, P., Rau, F., Raup, B., Rich, J., Rott, H., Sakai, A., Schneider, C., Seliverstov, Y., Sharp, M., Sigurðsson, O., Stokes, C., Way, R., Wheate, R., Winsvold, S., Wolken, G., Wyatt, F., and Zheltyhina, N.: Randolph Glacier Inventory 5.0: A dataset of global glacier outlines., Digital media, Global Land Ice Measurements from Space, Boulder Colorado, USA, https://www.glims.org/RGI/index.html, 2015.

Bao, W., Liu, S., Wei, J., and Guo, W.: Glacier changes during the past 40 years in the West Kunlun Shan, Journal of Mountain Science, 12, 344–357, https://doi.org/10.1007/s11629-014-3220-0, 2015.

Barandun, M., Huss, M., Usubaliev, R., Azisov, E., Berthier, E., Kääb, A., Bolch, T., and Hoelzle, M.: Multi-decadal mass balance series of three Kyrgyz glaciers inferred from modelling constrained with repeated snow line observations, The Cryosphere, 12, 1899-1919, https://doi.org/10.5194/tc-12-1899-2018, 2018.

Baumann, S.: Estimating glacier mass changes by GRACE satellite gravimetry in the Pamir and Tien-Shan mountains, Central Asia, in: 2012 IEEE International Geoscience and Remote Sensing Symposium, pp. 4461–4464, https://doi.org/10.1109/IGARSS.2012.6350481, 2012.

Berrisford, P., Dee, D., Poli, P., Brugge, R., Fielding, K., Fuentes, M., Kållberg, P., Kobayashi, S., Uppala, S., and Simmons, A.: The ERA-Interim archive Version 2.0, Shinfield Park, Reading, 2011.

Böhner, J.: General climatic controls and topoclimatic variations in Central and High Asia, Boreas, 35, 279–295, https://doi.org/10.1111/j.1502-3885.2006.tb01158.x, 2006.

Bolch, T., Kulkarni, A., Kääb, A., Huggel, C., Paul, F., Cogley, J. G., Frey, H., Kargel, J. S., Fujita, K., Scheel, M., Bajracharya, S., and Stoffel, M.: The State and Fate of Himalayan Glaciers, Science, 336, 310–314, https://doi.org/10.1126/science.1215828, 2012.

Bookhagen, B. and Burbank, D. W.: Topography, relief, and TRMM-derived rainfall variations along the Himalaya, Geophys. Res. Lett., 33, https://doi.org/10.1029/2006GL026037, 2006.

Bookhagen, B. and Burbank, D. W.: Toward a complete Himalayan hydrological budget: Spatiotemporal distribution of snowmelt and rainfall and their impact on river discharge, Journal of Geophysical Research: Earth Surface, 115, https://doi.org/10.1029/2009JF001426, 2010.

Bosilovich, M. G., Lucchesi, R., and Suarez, M.: MERRA-2: File Specification, Gmao office note no. 9 (version 1.1), Global Modeling and Assimilation Office, NASA Goddard Space Flight Center, Greenbelt, Maryland, USA, 2016.

Bothe, O., Fraedrich, K., and Zhu, X.: Precipitation climate of Central Asia and the large-scale atmospheric circulation, Theoretical and Applied Climatology, 108, 345–354, https://doi.org/10.1007/s00704-011-0537-2, 2012.

Brun, F., Berthier, E., Wagnon, P., Kääb, A., and Treichler, D.: A spatially resolved estimate of High Mountain Asia glacier mass balances from 2000 to 2016, Nature Geoscience, 10, 668–673, https://doi.org/10.1038/ngeo2999, 2017.

Cogley, J. G.: Present and future states of Himalaya and Karakoram glaciers, Annals of Glaciology, 52, 69–73, https://doi.org/10.3189/172756411799096277, 2011.

Cogley, J. G.: Climate science: Himalayan glaciers in the balance, Nature, 488, 468–469, https://doi.org/10.1038/488468a, 2012.

Dobhal, D., Mehta, M., and Srivastava, D.: Influence of debris cover on terminus retreat and mass changes of Chorabari Glacier, Garhwal region, central Himalaya, India, Journal of Glaciology, 59, 961–971, https://doi.org/10.3189/2013JoG12J180, 2013.

Farinotti, D., Longuevergne, L., Moholdt, G., Duethmann, D., Mölg, T., Bolch, T., Vorogushyn, S., and Güntner, A.: Substantial glacier mass loss in the Tien Shan over the past 50 years, Nature Geoscience, 8, 716–722, https://doi.org/10.1038/ngeo2513, 2015.

Farr, T. G. and Kobrick, M.: Shuttle radar topography mission produces a wealth of data, Eos, Transactions American Geophysical Union, 81, 583–585, https://doi.org/10.1029/EO081i048p00583, 2000.

Farr, T. G., Rosen, P. A., Caro, E., Crippen, R., Duren, R., Hensley, S., Kobrick, M., Paller, M., Rodriguez, E., Roth, L., Seal, D., Shaffer, S., Shimada, J., Umland, J., Werner, M., Oskin, M., Burbank, D., and Alsdorf, D.: The Shuttle Radar Topography Mission, Reviews of Geophysics, 45, https://doi.org/10.1029/2005RG000183, 2007.

Fujita, K.: Effect of precipitation seasonality on climatic sensitivity of glacier mass balance, Earth and Planetary Science Letters, 276, 14–19, https://doi.org/10.1016/j.epsl.2008.08.028, 2008.

Fujita, K. and Nuimura, T.: Spatially heterogeneous wastage of Himalayan glaciers, Proceedings of the National Academy of Sciences, 108, 14 011–14 014, https://doi.org/10.1073/pnas.1106242108, 2011.

Fujita, K., Takeuchi, N., Nikitin, S. A., Surazakov, A. B., Okamoto, S., Aizen, V. B., and Kubota, J.: Favorable climatic regime for maintaining the present-day geometry of the Gregoriev Glacier, Inner Tien Shan, The Cryosphere, 5, 539–549, https://doi.org/10.5194/tc-5-539-2011, 2011.

Gardelle, J., Berthier, E., and Arnaud, Y.: Impact of resolution and radar penetration on glacier elevation changes computed from DEM differencing, Journal of Glaciology, 58, 419–422, https://doi.org/10.3189/2012JoG11J175, 2012a.

Gardelle, J., Berthier, E., and Arnaud, Y.: Slight mass gain of Karakoram glaciers in the early twenty-first century, Nature Geoscience, 5, 322–325, https://doi.org/10.1038/ngeo1450, 2012b.

Gardelle, J., Berthier, E., Arnaud, Y., and Kääb, A.: Region-wide glacier mass balances over the Pamir-Karakoram-Himalaya during 1999–2011, The Cryosphere, 7, 1263–1286, https://doi.org/10.5194/tc-7-1263-2013, 2013.

Gardner, A. S., Moholdt, G., Cogley, J. G., Wouters, B., Arendt, A. A., Wahr, J., Berthier, E., Hock, R., Pfeffer, W. T., Kaser, G., Ligtenberg, S. R. M., Bolch, T., Sharp, M. J., Hagen, J. O., van den Broeke, M. R., and Paul, F.: A Reconciled Estimate of Glacier Contributions to Sea Level Rise: 2003 to 2009, Science, 340, 852–857, https://doi.org/10.1126/science.1234532, 2013.

GMAO: tavgM_2d_flx_Nx: MERRA 2D IAU Diagnostic Surface Fluxes, Monthly Mean V5.2.0. Accessed: Dec 1, 2016, Dataset, Goddard Space Flight Center Distributed Active Archive Center (GSFC DAAC), https://doi.org/10.5067/0JRLVL8YV2Y4, 2016.

Gilbert, A., Leinss, S., Kargel, J., Kääb, A., Gascoin, S., Leonard, G., Berthier, E., Karki, A. and Yao, T.: Mechanisms leading to the 2016 giant twin glacier collapses, Aru Range, Tibet, The Cryosphere, 12(9), 2883–290, https://doi.org/10.5194/tc-12-2883-2018, 2018.

Girod, L., Nuth, C., Kääb, A., McNabb, R. and Galland, O.: MMASTER: Improved ASTER DEMs for Elevation Change Monitoring, Remote Sensing, 9, Artn 704, https://doi.org/10.3390/rs9070704, 2017.

Gorelick, N., Hancher, M., Dixon, M., Ilyushchenko, S., Thau, D., and Moore, R.: Google Earth Engine: Planetary-scale geospatial analysis for everyone, Remote Sensing of Environment, https://doi.org/10.1016/j.rse.2017.06.031, 2017.

Guo, Y., Zhang, Y., Ma, N., Xu, J., and Zhang, T.: Long-term changes in evaporation over Siling Co Lake on the Tibetan Plateau and its impact on recent rapid lake expansion, Atmospheric Research, 216, 141-150, https://doi.org/doi.org/10.1016/j.atmosres.2018.10.006, 2019.

Hewitt, K.: The Karakoram Anomaly? Glacier Expansion and the 'Elevation Effect', Karakoram Himalaya, Mountain Research and Development, 25, 332–340, https://doi.org/10.1659/0276-4741(2005)025[0332:TKAGEA]2.0.CO;2, 2005.

Huss, M.: Density assumptions for converting geodetic glacier volume change to mass change, The Cryosphere, 7, 877–887, https://doi.org/10.5194/tc-7-877-2013, 2013.

Immerzeel, W. W., Petersen, L., Ragettli, S., and Pellicciotti, F.: The importance of observed gradients of air temperature and precipitation for modeling runoff from a glacierized watershed in the Nepalese Himalayas, Water Resources Research, 50, 2212–2226, https://doi.org/10.1002/2013WR014506, 2014.

Immerzeel, W. W., Wanders, N., Lutz, A. F., Shea, J. M., and Bierkens, M. F. P.: Reconciling high-altitude precipitation in the upper Indus basin with glacier mass balances and runoff, Hydrology and Earth System Sciences, 19, 4673–4687, https://doi.org/10.5194/hess-19-4673-2015, 2015.

Jacob, T., Wahr, J., Pfeffer, W. T., and Swenson, S.: Recent contributions of glaciers and ice caps to sea level rise, Nature, 482, 514–518, https://doi.org/10.1038/nature10847, 2012.

Kääb, A., Berthier, E., Nuth, C., Gardelle, J., and Arnaud, Y.: Contrasting patterns of early twenty-first-century glacier mass change in the Himalayas, Nature, 488, 495–498, https://doi.org/10.1038/nature11324, 2012.

Kääb, A., Treichler, D., Nuth, C., and Berthier, E.: Brief Communication: Contending estimates of 2003-2008 glacier mass balance over the Pamir-Karakoram-Himalaya, The Cryosphere, 9, 557–564, https://doi.org/10.5194/tc-9-557-2015, 2015.

Kääb, A., Leinss, S., Gilbert, A., Bühler, Y., Gascoin, S., Evans, S.G., Bartelt, P., Berthier, E., Brun, F., Chao, W.A., Farinotti, D., Gimbert, F., Guo, W.Q., Huggel, C., Kargel, J.S., Leonard, G.J., Tian, L.D., Treichler, D. and Yao, T.D. : Massive collapse of two glaciers in western Tibet in 2016 after surge-like instability, Nature Geoscience, 11, 114-120, https://doi.org/10.1038/s41561-017-0039-7, 2018.

Kang, S., Chen, F., Gao, T., Zhang, Y., Yang, W., Yu, W., and Yao T.: Correspondence: Early onset of rainy season suppresses glacier melt: a case study on Zhadang glacier, Tibetan Plateau, Journal of Glaciology, 55, 755–758, https://doi.org/10.3189/002214309789470978, 2009.

Kapnick, S.B., Delworth, T.L., Ashfaq, M., Malyshev, S., and Milly, P.C.D.: Snowfall less sensitive to warming in Karakoram than in Himalayas due to a unique seasonal cycle, Nature Geoscience, 7(11), 834–840, https://doi.org/10.1038/ngeo2269, 2014.

Ke, L., Ding, X., and Song, C.: Heterogeneous changes of glaciers over the western Kunlun Mountains based on ICESat and Landsat-8 derived glacier inventory, Remote Sensing of Environment, 168, 13–23, https://doi.org/10.1016/j.rse.2015.06.019, 2015.

Kenzhebaev, R., Barandun, M., Kronenberg, M., Chen, Y., Usubaliev, R., and Hoelzle, M.: Mass balance observations and reconstruction for Batysh Sook Glacier, Tien Shan, from 2004 to 2016, Cold Regions Science and Technology, 135, 76 – 89, https://doi.org/10.1016/j.coldregions.2016.12.007, 2017.

Kronenberg, M., Barandun, M., Hoelzle, M., Huss, M., Farinotti, D., Azisov, E., Usubaliev, R., Gafurov, A., Petrakov, D., and Kääb, A.: Mass-balance reconstruction for Glacier No. 354, Tien Shan, from 2003 to 2014, Annals of Glaciology, 57, 92–102, https://doi.org/10.3189/2016AoG71A032, 2016.

Kropáček, J., Braun, A., Kang, S.C., Feng, C., Ye, Q.H. and Hochschild, V: Analysis of lake level changes in Nam Co in central Tibet utilizing synergistic satellite altimetry and optical imager, International Journal of Applied Earth Observation and Geoinformation, 7, 3-11, https://doi.org/10.1016/j.jag.2011.10.001, 2012.

Kuhle, M.: The cold deserts of high Asia (Tibet and contiguous mountains), GeoJournal, 20, 319–323, https://doi.org/10.1007/BF00642997, 1990.

Lehner, B. and Döll, P.: Development and validation of a global database of lakes, reservoirs and wetlands, Journal of Hydrology, 296, 1–22, https://doi.org/10.1016/j.jhydrol.2004.03.028, 2004.

Lei, Y., T. Yao, B. W. Bird, K. Yang, J. Zhai, and Sheng. Y.: Coherent lake growth on the central Tibetan Plateau since the 1970s: characterization and attribution, Journal of Hydrology, 483, 61–67, https://doi.org/10.1016/j.jhydrol.2013.01.003, 2013.

Li, Z., Gao, Y., Wang, Y., Pan, Y., Li, J., Chen, A., Wang, T., Han, C., Song, Y. and Theakstone, W.: Can monsoon moisture arrive in the Qilian Mountains in summer?, Quaternary International, 358, 113–125, https://doi.org/10.1016/j.quaint.2014.08.046, 2015.

Matsuo, K. and Heki, K.: Time-variable ice loss in Asian high mountains from satellite gravimetry, Earth and Planetary Science Letters, 290, 30–36, https://doi.org/10.1016/j.epsl.2009.11.053, 2010.

Maussion, F., Scherer, D., Mölg, T., Collier, E., Curio, J., and Finkelnburg, R.: Precipitation Seasonality and Variability over the Tibetan Plateau as Resolved by the High Asia Reanalysis, Journal of Climate, 27, 1910–1927, https://doi.org/10.1175/JCLI-D-13-00282.1, 2014.

Mölg, T., Maussion, F., Yang, W., and Scherer, D.: The footprint of Asian monsoon dynamics in the mass and energy balance of a Tibetan glacier, The Cryosphere, 6, 1445–1461, https://doi.org/10.5194/tc-6-1445-2012, 2012.

Mölg, T., Maussion, F., and Scherer, D.: Mid-latitude westerlies as a driver of glacier variability in monsoonal High Asia, Nature Climate Change, 4, 68–73, https://doi.org/10.1038/nclimate2055, 2014.

Mukhopadhyay, B. and Khan, A.: A quantitative assessment of the genetic sources of the hydrologic flow regimes in Upper Indus Basin and its significance in a changing climate, Journal of Hydrology, 509, 549–572, https://doi.org/10.1016/j.jhydrol.2013.11.059, 2014.

Narama, C., Kääb, A., Duishonakunov, M., and Abdrakhmatov, K.: Spatial variability of recent glacier area changes in the Tien Shan Mountains, Central Asia, using Corona (1970), Landsat (2000), and ALOS (2007) satellite data, Global and Planetary Change, 71, 42–54, https://doi.org/10.1016/j.gloplacha.2009.08.002, 2010.

Neckel, N., Kropáček, J., Bolch, T., and Hochschild, V.: Glacier mass changes on the Tibetan Plateau 2003–2009 derived from ICESat laser altimetry measurements, Environmental Research Letters, 9, https://doi.org/10.1088/1748-9326/9/1/014009, 2014.

Nuth, C. and Kääb, A.: Co-registration and bias corrections of satellite elevation data sets for quantifying glacier thickness change, The Cryosphere, 5, 271–290, https://doi.org/10.5194/tc-5-271-2011, 2011.

Palazzi, E., von Hardenberg, J., and Provenzale, A.: Precipitation in the Hindu-Kush Karakoram Himalaya: Observations and future scenarios, Journal of Geophysical Research: Atmospheres, 118, 85–100, https://doi.org/10.1029/2012JD018697, 2013.

Pekel, J.-F., Cottam, A., Gorelick, N., and Belward, A. S.: High-resolution mapping of global surface water and its long-term changes, Nature, 540, 418–422, 10.1038/nature20584, 2016.

Pellicciotti, F., Stephan, C., Miles, E., Herreid, S., Immerzeel, W. W., and Bolch, T.: Mass-balance changes of the debris-covered glaciers in the Langtang Himal, Nepal, from 1974 to 1999, Journal of Glaciology, 61, 373–386, https://doi.org/10.3189/2015JoG13J237, 2015.

Phan, H. V., Lindenbergh, R., and Menenti, M.: Assessing orographic variability in glacial thickness changes at the Tibetan Plateau using ICESat laser altimetry, Remote Sensing, 9, https://doi.org/10.3390/rs9020160, 2017.

Pieczonka, T., Bolch, T., Junfeng, W., and Shiyin, L.: Heterogeneous mass loss of glaciers in the Aksu-Tarim Catchment (Central Tien Shan) revealed by 1976 KH-9 Hexagon and 2009 SPOT-5 stereo imagery, Remote Sensing of Environment, 130, 233–244, https://doi.org/10.1016/j.rse.2012.11.020, 2013.

Quincey, D. J., Braun, M., Glasser, N. F., Bishop, M. P., Hewitt, K., and Luckman, A.: Karakoram glacier surge dynamics, Geophysical Research Letters, 38, https://doi.org/10.1029/2011GL049004, 2011.

Ragettli, S., Bolch, T., and Pellicciotti, F.: Heterogeneous glacier thinning patterns over the last 40 years in Langtang Himal, Nepal, The Cryosphere, 10, 2075–2097, https://doi.org/10.5194/tc-10-2075-2016, 2016.

Ramanathan, A.: Status report on Chhota Shigri glacier (Himachal Pradesh), Himalayan glaciology technical report no.1, Department of Science and Technology, Ministry of Science and Technology, New Delhi, 2011.

Rasmussen, L. A.: Meteorological controls on glacier mass balance in High Asia, Annals of Glaciology, 54, 352–359, https://doi.org/10.3189/2013AoG63A353, 2013.

Rodriguez, E., Morris, C. S., and Belz, J. E.: A Global Assessment of the SRTM Performance, Photogrammetric Engineering & Remote Sensing, 72, 249–260, https://doi.org/10.14358/PERS.72.3.249, 2006.

Sakai, A., Nuimura, T., Fujita, K., Takenaka, S., Nagai, H., and Lamsal, D.: Climate regime of Asian glaciers revealed by GAMDAM glacier inventory, The Cryosphere, 9, 865–880, https://doi.org/10.5194/tc-9-865-2015, 2015.

Sakai, A., and Fujita, K.: Contrasting glacier responses to recent climate change in high-mountain Asia, Scientific Reports, 7, Artn. 13717, https://doi.org/10.1038/s41598-017-14256-5, 2017.

Salzmann, N., Huggel, C., Rohrer, M. and Stoffel, M.: Data and knowledge gaps in glacier, snow and related runoff research - A climate change adaptation perspective, Journal of Hydrology, 518, 225-234, https://doi.org/10.1016/j.jhydrol.2014.05.058, 2014.

Scherler, D., Bookhagen, B., and Strecker, M. R.: Spatially variable response of Himalayan glaciers to climate change affected by debris cover, Nature Geoscience, 4, 156–159, https://doi.org/10.1038/ngeo1068, 2011.

Schiemann, R., Lüthi, D., and Schär, C.: Seasonality and interannual variability of the Westerly Jet in the Tibetan Plateau region, Journal of Climate, 22, 2940–2957, https://doi.org/10.1175/2008JCLI2625.1, 2009.

Schutz, B. E., Zwally, H. J., Shuman, C. A., Hancock, D., and DiMarzio, J. P.: Overview of the ICESat Mission, Geophysical Research Letters, 32, https://doi.org/10.1029/2005GL024009, 2005.

Sen, P. K.: Estimates of the regression coefficient based on Kendall's tau, Journal of the American Statistical Association, 63, 1379–1389, https://doi.org/10.2307/2285891, 1968.

Shangguan, D., Liu, S., Ding, Y., Li, J., Zhang, Y., Ding, L., Wang, X., Xie, C., and Li, G.: Glacier changes in the west Kunlun Shan from 1970 to 2001 derived from Landsat TM/ETM+ and Chinese glacier inventory data, Annals of Glaciology, 46, 204–208, https://doi.org/10.3189/172756407782871693, 2007.

Shangguan, D. H., Bolch, T., Ding, Y. J., Kröhnert, M., Pieczonka, T., Wetzel, H. U., and Liu, S. Y.: Mass changes of Southern and Northern Inylchek Glacier, Central Tian Shan, Kyrgyzstan, during 1975 and 2007 derived from remote sensing data, The Cryosphere, 9, 703–717, https://doi.org/10.5194/tc-9-703-2015, 2015.

Sherpa, S. F., Wagnon, P., Brun, F., Berthier, E., Vincent, C., Lejeune, Y., Arnaud, Y., and Kayastha, R. B.: Contrasted Glacier Mass Wastage Between the Southern and the Inner Part of Everest Region Revealed from In-Situ Measurements since 2007, AGU Fall Meeting Abstracts 2016, 2016.

Shi, Y. and Liu, S.: Estimation on the response of glaciers in China to the global warming in the 21st century, Chinese Science Bulletin, 45, 668–672, https://doi.org/10.1007/BF02886048, 2000.

Shi, Y., Shen, Y., Kang, E., Li, D., Ding, Y., Zhang, G., and Hu, R.: Recent and future climate change in Northwest China, Climatic Change, 80, 379–393, https://doi.org/10.1007/s10584-006-9121-7, 2007.

Song, C.Q., Huang, B. and Ke, L.H.: Modeling and analysis of lake water storage changes on the Tibetan Plateau using multi-mission satellite data, Remote Sensing of Environment, 135, 25–35, https://doi.org/10.1016/j.rse.2013.03.013, 2013.

Song, C.Q., Huang, B. and Ke, L.H.: Heterogeneous change patterns of water level for inland lakes in High Mountain Asia derived from multi-mission satellite altimetry, Hydrological Processes, 29(12), 2769–2781, https://doi.org/10.1002/hyp.10399, 2015.

Sorg, A., Bolch, T., Stoffel, M., Solomina, O., and Beniston, M.: Climate change impacts on glaciers and runoff in Tien Shan (Central Asia), Nature Clim. Change, 2, 725–731, https://doi.org/10.1038/nclimate1592, 2012.

Sun, J., and Zhang, F.Q.: Daily extreme precipitation and trends over China, Science China-Earth Sciences, 60(12), 2190–2203, https://doi.org/10.1007/s11430-016-9117-8, 2017.

Tao, H., Gemmer, M., Bai, Y., Su, B., and Mao, W.: Trends of streamflow in the Tarim River Basin during the past 50 years: Human impact or climate change?, Journal of Hydrology, 400, 1–9, https://doi.org/10.1016/j.jhydrol.2011.01.016, 2011.

Tao, H., Borth, H., Fraedrich, K., Su, B., and Zhu, X.: Drought and wetness variability in the Tarim River Basin and connection to large-scale atmospheric circulation, International Journal of Climatology, 34, 2678–2684, https://doi.org/10.1002/joc.3867, 2014.

Theil, H.: A rank-invariant method of linear and polynomial regression analysis. Parts I, II, III, Proceedings of the Koninklijke Nederlandse Akademie van Wetenschappen, 53, 386–392, 521–525, 1397–1412, 1950.

Tian, H., Yang, T., and Liu, Q.: Climate change and glacier area shrinkage in the Qilian mountains, China, from 1956 to 2010, Annals of Glaciology, 55, 187–197, https://doi.org/10.3189/2014AoG66A045, 2014.

Treichler, D. and Kääb, A.: ICESat laser altimetry over small mountain glaciers, The Cryosphere, 10, 2129–2146, https://doi.org/10.5194/tc-10-2129-2016, 2016.

Treichler, D. and Kääb, A.: Snow depth from ICESat laser altimetry — A test study in southern Norway, Remote Sensing of Environment, 191, 389–401, https://doi.org/10.1016/j.rse.2017.01.022, 2017.

Vijay, S. and Braun, M.: Elevation change rates of glaciers in the Lahaul-Spiti (Western Himalaya, India) during 2000–2012 and 2012–2013, Remote Sensing, 8, 1038, https://doi.org/10.3390/rs8121038, 2016.

Wagnon, P., Vincent, C., Arnaud, Y., Berthier, E., Vuillermoz, E., Gruber, S., Ménégoz, M., Gilbert, A., Dumont, M., Shea, J. M., Stumm, D., and Pokhrel, B. K.: Seasonal and annual mass balances of Mera and Pokalde glaciers (Nepal Himalaya) since 2007, The Cryosphere, 7, 1769–1786, https://doi.org/10.5194/tc-7-1769-2013, 2013.

WGMS: Fluctuations of Glaciers Database, Digital data, World Glacier Monitoring Service, Zurich, Switzerland, https://doi.org/10.5904/wgms-fog-2016-08, 2016.

Yao, T., Thompson, L., Yang, W., Yu, W., Gao, Y., Guo, X., Yang, X., Duan, K., Zhao, H., Xu, B., Pu, J., Lu, A., Xiang, Y., Kattel, D. B., and Joswiak, D.: Different glacier status with atmospheric circulations in Tibetan Plateau and surroundings, Nature Climate Change, 2, 663–667, https://doi.org/10.1038/nclimate1580, 2012.

Yi, S. and Sun, W.: Evaluation of glacier changes in high-mountain Asia based on 10 year GRACE RL05 models, Journal of Geophysical Research: Solid Earth, 119, 2504–2517, https://doi.org/10.1002/2013JB010860, 2014.

Zhang, G., Xie, H., Kang, S., Yi, D., and Ackley, S. F.: Monitoring lake level changes on the Tibetan Plateau using ICESat altimetry data (2003–2009), Remote Sensing of Environment, 115, 1733–1742, https://doi.org/10.1016/j.rse.2011.03.005, 2011.

Zhang, G., Yao, T., Xie, H., Kang, S., and Lei, Y.: Increased mass over the Tibetan Plateau: from lakes or glaciers?, Geophysical Research Letters, 40, 2125–2130, https://doi.org/10.1002/grl.50462, 2013.

Zhang, G., Yao, T., Shum, C. K., Yi, S., Yang, K., Xie, H., Feng, W., Bolch, T., Wang, L., Behrangi, A., Zhang, H., Wang, W., Xiang, Y., and Yu, J.: Lake volume and groundwater storage variations in Tibetan Plateau's endorheic basin, Geophysical Research Letters, 44, 5550–5560, https://doi.org/10.1002/2017GL073773, 2017.

Zhang, Y., Hirabayashi, Y., and Liu, S.: Catchment-scale reconstruction of glacier mass balance using observations and global climate data: Case study of the Hailuogou catchment, south-eastern Tibetan Plateau, Journal of Hydrology, 444–445, 146–160, https://doi.org/10.1016/j.jhydrol.2012.04.014, 2012.

Zwally, H., Schutz, R., Hancock, D., and Dimarzio, J.: GLAS/ICESat L2 Global Land Surface Altimetry Data, Versions 33/34, GLAH14, Dataset, NASA DAAC at the National Snow and Ice Data Center, Boulder, Colorado USA, https://doi.org/10.5067/ICESAT/GLAS/DATA207, 2012.